

# LIBRARY Michigan State University

This is to certify that the

thesis entitled

Geochemistry of the Lower Keweenawan

Powder Mill Group, Upper Michigan

presented by

James Walter Gell

has been accepted towards fulfillment of the requirements for

Master's degree in Geology

Major professor

Date \_\_\_\_\_



MSU LIBRARIES RETURNING MATERIALS:
Place in book drop to
remove this checkout from
your record. FINES will
be charged if book is
returned after the date
stamped below.

1 pt 5 0 909

# GEOCHEMISTRY OF THE LOWER KEWEENAWAN POWDER MILL GROUP, UPPER MICHIGAN

Ву

James Walter Gell

# A THESIS

Submitted to
Michigan State University
in partial fulfillment of the requirements
for the degree of

MASTER OF SCIENCE

Department of Geology

1987

#### **ABSTRACT**

# GEOCHEMISTRY OF THE LOWER KEWEENAWAN POWDER MILL GROUP, UPPER MICHIGAN

By

#### James Walter Gell

The Powder Mill Group (PMG) in upper Michigan is comprised of the Siemens Creek Formation and the Kallander Creek Formation. The Siemens Creek flows represent the first accumulation of lavas related to the opening of the Keweenawan Rift system approximately 1.2 Ga. The basal flows are primitive Mg-rich whereas the remainder of the pile (1300 m) is predominantly tholeitic basalt and small volumes of andesite. These rocks have distinct trends in process identification diagrams which are consistent with partial melting.

The overlying Kallander Creek Formation contains a greater volume of more evolved basalts and andesites through the 1200 m of exposed section. These have distinctly different trends than the Siemens Creek lavas. The Kallander Creek lavas plot as trends consistent with fractional crystallization in the process identification diagrams. The variation of major element abundances in end members can be derived by up to 40% crystal fractionation of olivine, pyroxene, and plagioclase.

The sequence of magmatic events recorded in the PMG is consistent with previous models proposed for opening of the Keweenawan Rift.

Downward propagating fractures provided conduits for magma generated by partial melting of the mantle. These magmas are represented by the more primitive Siemens Creek lavas. Ponding and subsequent fractionation of magmas in the upper crust followed and is represented by the Kallander Creek lavas.

# TABLE OF CONTENTS

LIST OF TABLES	. v
LIST OF FIGURES	. vi
INTRODUCTION	. 1
REGIONAL GEOLOGIC SETTING	. 6
STUDY LOCATION	. 7
PETROGRAPHY	. 9
MAJOR, TRACE AND RARE EARTH ELEMENT CHEMISTRY	. 14
MAJOR ELEMENTS	. 14
REE and TRACE ELEMENTS	. 22
PETROGENETIC MODELING	. 36
RESULTS	. 44
APPENDIX A: ANALYTICAL METHODS	. 47
APPENDIX B: INSTRUMENTATION	. 48
I IST OF REFERENCES	49

# LIST OF TABLES

Table 1	Chemical Data for the Powder Mill Group Lavas	15
Table 2	Process Identification Diagram Intercept Calculations	39
Table 3	Multiple Linear Regression Analysis Calculations	42

# LIST OF FIGURES

Figure 1	Location Map
Figure 2	Rb - Sr Isochron
Figure 3	AFM Ternary Diagram
Figure 4	Nb-Zr-Y Diagram
Figure 5	Variation Diagrams
Figure 6	REE Chondrite-Normalized Plots
Figure 7	Process Identification Diagrams
Figure 8	"Spider" Plots
Figure 9	Nb* Plot [(Th <sub>n</sub> + La <sub>n</sub> ) - Nb <sub>n</sub> ) v. FeO/(FeO+MgO)] 33
Figure 10	Element Variation with Stratigraphic Height

#### INTRODUCTION

The Lower Keweenwan age Powder Mill Group (PMG) represents the first lavas extruded in Michigan as part of the Midcontinent rift (MCR). The extent of the MCR, also known as the Keweenawan Rift, is defined by the Midcontinent Geophysical Anomaly (O'Hara, 1982) that extends from northeastern Kansas, through the Lake Superior Region, and south to central Tennessee. The rocks of the MCR are exposed only in the Lake Superior Region.

As the eruptive product of a major continental rifting event, the rocks of the PMG reflect the characteristics of their Middle Proterozoic mantle source. This study is the first detailed geochemical and petrogenetic characterization of rocks related to the early stages of the Keweenawan rift in Michigan. The geochemistry of the lavas reflect the processes of an evolving magmatic system of the rift. Models for the MCR proposed in previous publications (Gordon and Hempton, 1986; Miller, 1986; and Green 1983) are the result of extensive studies of the Keweenawan intrusive and extrusive rocks of Minnesota, Wisconsin, and Ontario. The results of this investigation are used to evaluate these models to determine if they have an application for the Michigan rocks.

The PMG extends more than 160 km from southern Houghton County in Michigan westward to Grandview, Wisconsin (Wasuwanich, 1979). This study encompasses the eastern half of its extent as illustrated in Figure 1.

Previous work on the Lower Keweenawan rocks of Northern Michigan and Wisconsin has been limited to geologic mapping, descriptions, and

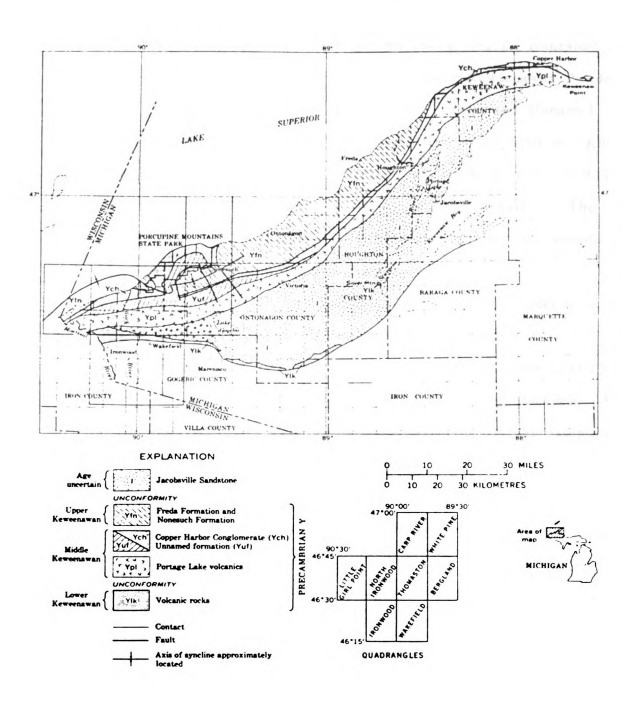


Figure 1 Location Map

limited geochemical analyses. The lavas were originally correlated with the Middle Keweenawan lavas (South Range Traps, Irving, 1883). Hubbard (1975) identified three groups of volcanics; the Lower Keweenawan Powder Mill Group, the Middle Keweenawan Portage Lake Lavas, and Unnamed Volcanics. In Michigan the thickness of the PMG is about 6100 m. Rb-Sr isotope data for the PMG (Wilband, 1984) give an initial Sr ratio of 0.7043 +/- 0.0003 and an age of 1209 +/- 36 Ma, as shown in Figure 2. The Keweenawan lavas are believed to related genetically to the dike swarms observed throughout the Lake Superior region.

The PMG is divided into two formations. The Siemens Creek

Formation is mostly tholeiitic basalts and some andesite flows that

conformably overly the Bessemer Quartzite, a Lower Keweenawan quartz

arenite (Hubbard, 1975). These lavas total about 1300 m in thickness. The

lavas are characterized by a reversed magnetic polarity with the exception

of the basal 130 m which are normally polarized (Books, 1972). Palmer and

Halls (1985) have suggested the normally polarized lavas were reversely

polarized at the time of their extrusion and subsequently reset during a

period of low grade metamorphism.

Lavas of the overlying Kallander Creek Formation have been characterized as basalts, and esites, and rhyodacites based on calculated norms (Hubbard, 1975). About 1200 m of the Kallander Creek lavas are exposed at the surface. These rocks have reverse magnetic polarity (Books, 1972).

The stratigraphic relationship of the Siemens Creek and the Kallander Creek is obscured by poor exposures along their contact although locally the contact is defined by a diorite sill (Hubbard, 1975).

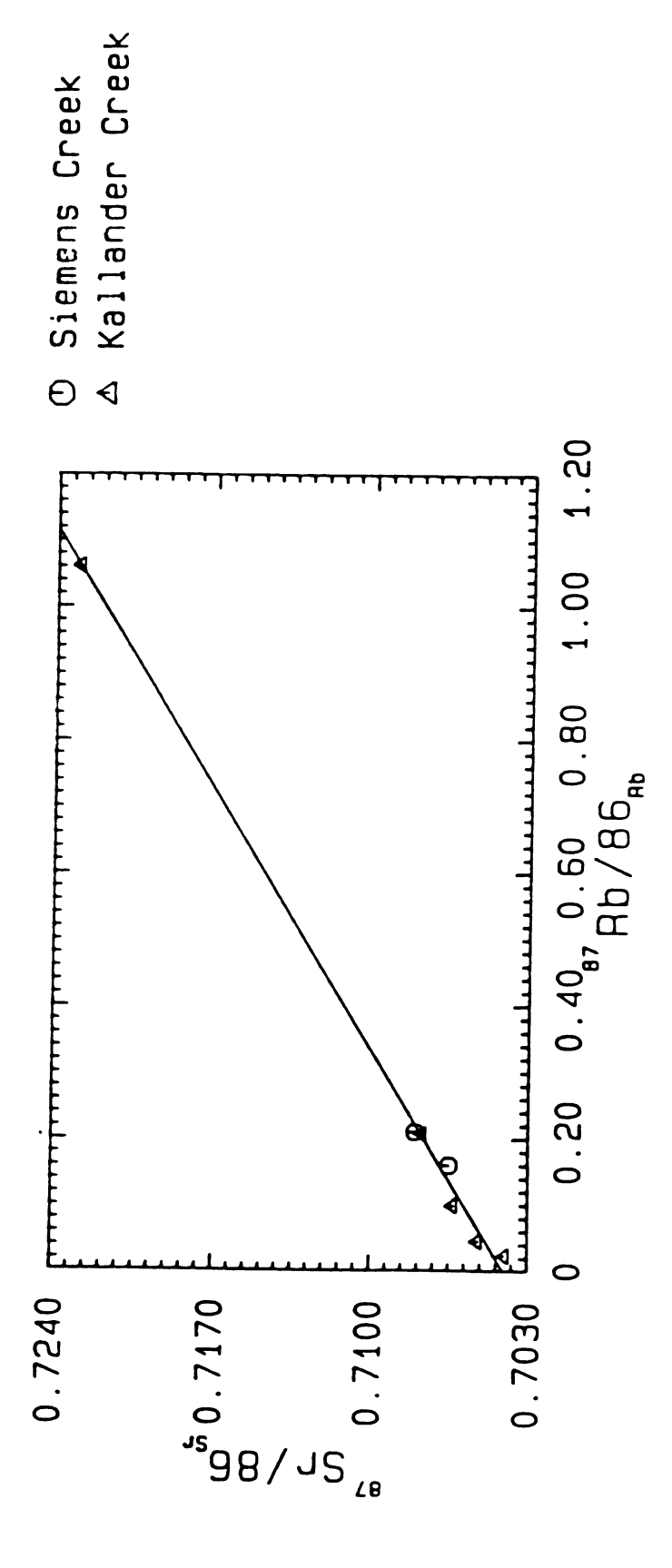


Figure 2 Rb - Sr Isochron

All the PMG lavas were subaerially extruded with the exception of the lowermost flows of the Siemens Creek which are pillowed (Green, 1982).

#### REGIONAL GEOLOGIC SETTING

Gordon and Hempton (1986) recently proposed a model for the origin of the MCR. They interpret the rift to be a series of pull-apart basins. These basins were generated by offsets along strike-slip faults that propagated as a result of the Grenville orogeny. Tensional tectonic forces associated with collision were sufficient to cause decompressive melting. Attenuation of the crust allowed the magmas to reach the surface through faults. This orogenic event controlled the location and duration of magmatic activity.

Green (1983) identified the pattern of Keweenawan volcanism in the Lake Superior Region as consisting of nine temporally and spatially separate eruptive basins. This is consistent with magmatic activity associated with pull-apart basins as presented by Gordon and Hempton (1986).

Miller (1986) examined the intrusive and related extrusive Keweenawan rocks of the Duluth Complex. A three stage model consisting of an early volcanism stage, an anorthitic stage, and a troctolitic stage is presented.

The rocks of the PMG are similar to Miller's (1986) the early volcanism stage.

Modeling of magnetic data by King (1975) indicates that a significant volume of Lower Keweenawan rocks, stratigraphically above the Kallander Creek Formation, are not exposed. The model represents a series of steeply dipping layers that are progressively deeper to the north, beyond the exposed rocks.

## STUDY LOCATION

The PMG lavas were sampled from the Wisconsin border east about 60 km to the Bond Falls Storage Basin (Figure 1). With the exception of the flat lying eastern exposures, the lavas dip steeply to the north with positive relief. This provides excellent sampling opportunities along the section. The extent of the lavas along strike also permits good lateral sampling. A total of 44 samples were selected for thin-section and chemical analysis. Of these 22 were from the Siemens Creek Formation, 21 from the Kallander Creek Formation, and 1 from the diorite sill. The lower 30 meters of the Siemens Creek are represented by 10 samples from several locations along strike. The remaining 12 samples are from continuous outcroppings that extend across the section. The Kallander Creek samples were collected from four positions along strike. A total of about 3000 meters of the PMG were sampled.

Basal flows and the Lower Siemens Creek lavas were sampled from the Bond Falls area where exposures of pyroxene-phyric basal pillow lavas are found along the northern shore of the storage basin. The lavas occur as oblate pillows about 20 to 40 cm in length. Four samples were collected from this location.

Southeast of Lake Gogebic, the basal 40 m of the flat lying Siemens

Creek lavas are exposed on a discontinuous cliff face. This section includes
the basal contact with the Bessemer Quartzite. The pillow lavas are
observed here as a deeply weathered zone extending 5 to 10 m above the
basal contact. Above this zone they give way to relatively fresh massive

flow units. These better preserved lavas continue to the top of the exposed section in this area. Four samples were collected from these outcrops.

Basal Siemens Creek lavas were also sampled at Mt. Zion in Ironwood.

The pillow lavas here are not pyroxene-phyric. This location is represented by two samples.

An additional twelve samples of the Siemens Creek lavas were obtained from outcrops north of the town of Bessemer. These outcrops provide a nearly continuous exposure of the lavas across section along which 1000 m of section was sampled at approximate 100 m intervals.

The Kallander Creek lavas were sampled at five locations up-section from the Siemens Creek exposures north of Bessemer. Samples were collected at irregular intervals comprising about 1500 meters of section.

The Kallander Creek lavas were also sampled along nearly vertically dipping exposures of the type section in the Powder Mill Creek. This section provided the most continuous exposure of the Kallander Creek lavas of which about 1200 m of section was sampled at six locations at approximate 200 m intervals.

Kallander Creek samples were also obtained from outcrops on the Powderhorn ski hill and from outcrops about 4 km northwest of Ironwood.

These five rocks represent the stratigraphically highest lavas sampled in the PMG.

An outcrop of Kallander Creek lavas was sampled at Gabbro Falls. A series of five consecutive flows were sampled. These flows are each about 15 m thick. Fine grained, vesicle free samples were taken from approximate flow centers.

### **PETROGRAPHY**

Detailed petrographic and microprobe analyses of the basal pillow lavas of the Siemens Creek Formation from the eastern part of the study area were made by Mattson et al. (1986). These lavas contain phenocrysts of Cr-rich pyroxene, serpentinized pseudomorphs after olivine phenocrysts, and chromite grains in a matrix of pyroxene, plagioclase, magnetite, and ilmenite.

The olivine pseudomorphs occur as euhedral to subhedral grains about 1 to 8 mm in diameter. The chromite crystals occur as euhedral to subhedral grains, about 0.06 mm in diameter. They are usually located within the altered olivines but some are found in the pyroxene phenocrysts.

Three pyroxene morphologies are present in the basal flows: anhedral matrix pyroxenes < 0.5 mm, 3 to 6 mm clusters of fine grained anhedral pyroxenes bounded by larger subhedral grains, and euhedral to subhedral phenocrysts 2 to 4 mm some of which are sector zoned (Mattson et al., 1986).

The size and abundance of the pyxroxene phenocryst and the presence of olivine in the pillow lavas are not seen in any of the later lavas. Miller (1986) and Green (1983) have observed the same sequence in the first Keweenawan lavas in Minnesota. They suggest these mafic rich lavas represent magmas generated by partial melting of a spinel lherzolite upper mantle (40 to 105 km). According to Miller (1986) pyroxene, olivine, and plagioclase were on the liquidus before tensional fracturing of the crust

associated with the MCR reached the magma. The magma erupted rapidly by the resulting release of pressure. The force of the eruption was sufficient to incorporate some of the cumulate phenocrysts. Later eruptives lack the large phenocrysts as a result of the developing "plumbing system" and erupted to the surface without incorporating these cumulate phenocrysts.

Visual estimations indicate the remainder of Siemens Creek lavas generally contain a greater if not equal amount of pyroxene than plagioclase. Pyroxene makes up between 40 to 65 modal percent and plagioclase 15 to 55 modal percent of the rock. Phenocrysts of both plagioclase and pyroxene are generally equigranular and are about 0.05 mm in length. Plagioclase crystal exhibit euhedral to subhedral form. Pyroxene grains are generally subhedral to anhedral.

A bimodal pyroxene grain size distribution is observed in three of the Siemens Creek flows. The smaller pyroxenes (~ 0.005 mm) often occur as clusters of small anhedral crystals surrounded by more coarse plagioclase laths. This reflects a magma in which plagioclase and pyroxene are on the liquidus with an interstitial pyroxene liquid that was quenched upon eruption.

Opaque minerals account for less than 5 modal percent of the rock.

One sample is observed to contain 20 percent opaque minerals. They are fined grained and generally anhedral although several samples contain euhedral crystals. In many of the samples the opaque minerals appear to occur in clusters and are often in close proximity to pyroxene crystals.

Apatite occurs in trace amounts as an accessory mineral in some of the Siemens Creek samples.

All of the Siemens Creek samples exhibit some degree of alteration.

The most common alteration product is chlorite occurring as up to 20 percent of the rock, though generally found as less than 5 modal percent.

The chlorite occurs most often at a grain boundary between pyroxene and the opaque minerals.

Other alteration products include pyroxene altering to biotite and plagioclase altering to sericite. Biotite occurs in quantities of up to 5 modal percent but is generally less than 1 percent. Sericite alteration is limited to less than 5 percent of the rock.

Quartz and calcite occur as secondary minerals in small amygdaloidal cavities in two of the Siemens Creek samples and are generally less than 0.005 mm in diameter.

Small pyroxene grains (~ 0.005 mm) often occur as clusters surrounded by or embedded in plagioclase grains. The petrogenetic implications of the pyroxene clusters is not clear. They may represent an increased rate of cooling that resulted in numerous nucleation sites in a pyroxene liquid trapped between plagioclase crystals. They may also be the product of plagioclase crystals acting as nucleation sites for the pyroxene crystals.

A small number of samples have ophitic and sub-ophitic textures.

These textures indicate pyroxene crystallized as an interstitial fluid around plagioclase crystals. Some of the larger plagioclase grains exhibit poikolitic textures. Small pyroxenes within the laths indicate a trapped pyroxene liquid during plagioclase crystallization.

The Kallander Creek lavas contain a greater proportion of plagioclase than pyroxene which is reflected in their higher bulk rock Al<sub>2</sub>O<sub>3</sub> content. By visual estimation the later lavas contain increasing modal percentages of plagioclase and less pyroxene. Plagioclase abundance varies from 50 to 85 modal percent while pyroxene varies from about 5 to 35 percent.

modal percent while pyroxene varies from about 5 to 35 percent.

Plagioclase and pyroxene crystals in the Kallander Creek lavas are equigranular and grain sizes range from 0.05 mm to 0.002 mm, generally smaller than those of the Siemens Creek. Grain size appears to vary inversely with the relative proportion of plagioclase; the plagioclase dominated flows exhibiting uniformly small crystals.

Glomeroporphyritic flows found in the upper-most exposures of the Kallander Creek Formation known as the "turkey track" lavas. These flows consist of coarse grained feldspar phenocrysts, about 5 mm to 10 mm in length, in a fine grained plagioclase matrix. Minor amounts of opaque minerals and pyroxene are also present.

Miller (1986) notes that plagioclase in basaltic liquids under pressure conditions of 8 to 10 kb are buoyant. This may account for the increasing abundance of plagioclase in the PMG lavas. The development of a plagioclase rich zone at the top of a fractionating magma chamber could provide the mafic poor liquids seen in the "turkey track" lavas.

In several of the Kallander Creek samples plagioclase phenocrysts exhibit oscillatory zoning, indicating growth in a dynamic magmatic environment. Albite twinning is evident in most plagioclase grains in the PMG. In some of the Kallander Creek lows a small number of grains exhibit Carlsbad twins.

The opaque minerals make up a minor proportion of the modal mineralogy. They occur as fine grained euhedral and subhedral crystals and form about 5 to 15 modal percent of the rock.

The fine grained texture of the Kallander Creek lavas made the identification of accessory minerals difficult. Rutile was often associated with chlorite alteration. Zircon and apatite were observed in some of the

plagioclase grains.

Variable amounts of alteration minerals are also present. Chlorite is the most abundant, comprising up to 20 percent of some samples. Sericite is locally an alteration product after plagioclase. Some samples contain biotite as an alteration product adjacent to opaque grains.

The alteration processes do not appear to have had a significant effect on trace element distribution as there is no apparent correlation between the degree of alteration and trace element concentrations.

# MAJOR, TRACE AND RARE EARTH ELEMENT CHEMISTRY

## MAJOR ELEMENTS

The rocks of the Siemens Creek are tholeilitic basalts. Major oxide abundances range from 54.5% to 47.7% SiO<sub>2</sub>; 13.7% to 2.2% MgO; 11.6% to 4.2% CaO; and 4.1% to 1.0% Na<sub>2</sub>O. Complete major element data are listed in Table 1. A ternary AFM plot for the PMG lavas is given in Figure 3. Their distribution in the AFM diagram correlates with those observed by Green (1982) in the North Shore Volcanic Group. Most of the lavas are in the tholeilite field as defined by Irving and Barager (1971) but a few of the Kallander Creek samples are in the calk-alkaline field. A Nb-Zr-Y discrimination diagram after Meschede (1986) for the PMG is given in Figure 4. The Siemens Creek flows fall in the "within-plate tholeilite" region whereas the Kallander Creek flows lie in the "within-plate alkali basalt" field. Both Formations show an enrichment in Zr. Although there is a variation in the major oxides, there is no simple correlation with stratigraphic position.

The basal Siemens Creek lavas are the most primitive of the suite.

They have the highest values of compatible elements such as MgO, CaO, Ni, and Cr as well as the lowest incompatible element values such as SiO<sub>2</sub>, Th, La, and Zr. The upper flows of the Kallander Creek lavas are the most evolved with low compatible element values and high incompatible element values. Previous work by Wasuwanich (1979) identified two chemically distinct groups of rocks in the Keweenawan diabase dikes and Portage Lake Lavas based on P<sub>2</sub>O<sub>5</sub>, Al<sub>2</sub>O<sub>3</sub>, TiO<sub>2</sub>, and REE. The bimodal distribution

Table 1 Chemical Data for the Powder Mill Group Lavas

AP-10	AF-12	AP-15	APISA	M1 2F	MM-3	MW-3A	7 3 1 4 4 4 4 4 4 4 4 4 4 4 4 4 4 4 4 4 4	N-3E	SC-2	HT2	JB-1
10 T	47.82	48.4	47.73	50.17	52.36	64.69	30.55	53.03	53.54	51.94	50.05
1.93	1.39	1.86	1.78	1.71	1.86	1.89	1.8	2.16	1.18	1.79	1.8
11.14	9.52	10.36	10.81	14.8	12.56	12.04	10.97	12.64	14.08	11.87	14.02
•	0	•	9	9	0	9	0	0	0	၁	၁
12.92	12.06	12.08	11.49	10.58	12.28	12.03	12.15	12.35	10.49	10.86	11.4
0.13	0.18	0.14	0.14	Ú. 17	0.19	c. 19	0.23	0.18	0.17	0.16	0.16
13.2	13.71	12.07	12.02	6.31	8.46	7.59	11.04	6.52	6.28	8.7	^
6.6	8.83	9.55	10.04	8.42	9.16	8.67	11.57	9.87	9.28	8.3	9.56
1.11	10.1	1.08	1.09	3.03	2.93	3.27	1.39	2.1	3.02	1.86	1.7
0.13	0.63	0.13	0	1.53	1.04	0.46	•	Ċ. 92	1.08	1.04	1.46
0.19	0.16	0.18	0.17	0.24	0.18	0.18	0.19	0.2	0.17	0.17	0.18
423.7	604.3	477.7	404.0	105.9	1 661	176.1	393.4	95.7	4	144.5	110.9
210.8	134.1	135.6	139.3	129.2	94.7	103.5	121.5	40	94.1	94.7	137.9
103.6	93.8	98.9	94.6	47.7	102.6	103.9	91.5	105.7	93.6	104.9	98.1
P)	11	и. В	- - -	27.9	18	٠. د.	4.6	17.2	20.1	18.1	33.9
204.8	236.7	224.9	227.4	768.2	374.6	201.2	220.8	291.1	214.5	393.3	192.1
20.1	19.7	21.1	19	24.6	22.1	20.8	20.7	25.1	24.7	23	25.9
135.6	118.3	138.4	129.1	180.5	157.3	151.3	128.1	185.7	140.8	155.6	138.2
9.8	6.9	7	7.9	6.57	ρ. 3.	9.4	7.3	8.3	16.1	6.5	7.4
13.0	12.9	13.6	14.2	6.	17.0	14.6	19.1	17.0	22.6	15.2	. n
38.7	33.5	41.5	41.4	46.8	31.4	37.4	42.1	47.5	51.6	38.8	38.9
	7.1	4.	4.9	υ (4	4.6	4.6	4.0	5.7		4.9	4.4
1.9	1.4	1.6	1.9	2.0	1.5	1.9	9:1	2.1	1.6	1.8	1.6
0.0	0.0	1.1	9.0	 	6.0	6.0	<b>∞</b> .≎	<b>9.</b> 0	6.7	1.2	1.1
1.7	1.7	1.9	1.1	٠.	2.0	6.1	1.8	2.5	2.1	2.0	r) (4
♦.0	0.2	o. u	o. 0	0.5	n.0	<b>6.</b> 0	<b>₹</b> .0	o. 0	•••	♦.0	0.4
u.5	2.7	o.p	d.b	n.	4.7	o.4	3.6	A. W.	4.4	a.8	4.6
1.1	0.0	0.7	0.7	-:	1.7	0.1	6.0	1.2	м. В.	2.3	1.9
941.7	1152.5	971.6	1006.6	212.8	410.1	327.8	844.0	227.9	117.5	429.3	278.9

Table 1 (Cont'd.)

¥-0x	51.73	2.86	15.92	C	12.57	0.16	4.03	40.04	3.52	2.62	0.33	4.6	24.5	13.6	39.3	134	34	395.7	26.1	66.0	136.9	11.4	4.0	1.3	2.7	0.3	O.8	6.4	0.0
B-7	49.67	2.61	14.55	0	13.91	0.0	3.97	10.13	~	0.69	0.27	115.3	272.8	100.6	22.5	164.7	44.4	233.2	13.7	19.2	30.5	7.0	2.4	1.6	4.4	0.0	6. S	2.6	203.9
۲- <b>۵</b>	48.43	3.28	12.99	0	13.9	0.24	80.9	0.0	1.89	0.0	0.43	84.6	217.2	118.4	17.0	210.8	46.5	277	17.1	22.7	91.19	9.8	2.7	r. 5	€.	o.8	7.4	- n	135.2
90-1	48.42	4.4	13.08	0	16.91	0.24	5.83	9.93	2.07	0.59	0.48	84.3	260.4	121	13.1	199.2	47.6	289.4	14.3	26.5	67.4	8.7	2.7	2.0	o.0	0.1	7.8	4.7	142.4
<b>G</b>	51.7	1.27	15.79	•	11.11	0.19	7.54	9.53	2.1	0.63	0.13	93	100.8	9°.6	16.2	447.6	23.5	125.8	6.6	18.3	33.7	4.0	n:-	9.C	2.3	0.3	- m	0 ri	189.7
8-8	50.53	1.93	14.78	c	12.67	0.19	6.13	10.18	2.39	0.96	0.21	110.2	164.4	01.10 1.13	17.5	287.1	26.7	133	9.6	16.0	39.2	4. 9.	9.	n .	2.0	0.4	2.9	2.5	121.4
. <b>.</b>	52.29	1.1	14.77	c	10.89	0.17	7.43	10,37	1.85	0.99	0.13	129.4	98.7	85.3	26.4	291.3	23.2	102.4	6.1	15.8	26.5	3.4	1.3	0.0	1.7	6.0	2.5	ر. ت	177.0
B-4	54.52	1.4	14.63	9	10.61	0.16	<b>8</b>	9.23	2.32	1.02	0.21	64.7	225.1	97.4	17.7	330.3	22.9	160.3	11.7	27.0	47.1	o.0	1.7	0.7	6.1	0.3	3.7	4.6	91.1
B-2A	51.52	1.72	14.47	0	12.09	0.16	7.42	4.6	1.79	1.23	0.5	127.1	97.5	78.6	21.9	267.6	23.4	141	13.7	18.7	43.2	4.4	1.6	9.0	1.6	0.4	2.9	2.1	81.5
B-2	51.61	1.64	14.81	c	11.55	0.16	7.03	9.68	1.98	1.31	0.22	132.2	118.2	80.2	23.7	292.4	24.2	159.3	16.4	21.3	47.8	4.5	1.8	1.0	1.9	n.0	7.0	3.3	92.9
B-1A	50.38	1.95	15.58	0	12.93	0.16	5.83	9.75	2.17	0.49	0.24	121.1	191.5	106.2	18.8	300.9	27.4	144.1	o. 0	16.4	41.5	4.7	2.0	·-	2.0	0.4	, ,	7.7	121.3
1-8	51.88	1.78	13.1	c	10.01	0.18	6.3	8.84	3.01	1.33	0.25	115.8	108.9	97.1	24.4	377.6	23.5	161.5	17.5	24.7	52.3	4.7	1.7	<b>0.</b> 0	1.2	0.3	3.6	1.1	226.0
	2102	1102	A1203	Fe203	0	J.	Н90	040	N.20	K20	F205	ž	3	٧2	æ	ຮ	>	<b>7</b>	ş	•	ů	<b>e</b> S	Fu	2	٩ ۲	3	Ĭ	Ę	ր

Table 1 (Cont'd.)

												•																	
												111.9																	
89 1	52.03	3.79	14.13	O	14.12	0.1	4.97	4.00	G.50	2.36	0.66	48.8	178.	17:	69.	948.	48.6	496.	38.	73.	149.	.03	'n	_	'n	•	•	7.	(
K-7	51.42	3.43	11.96	•	18.23	0.19	3.6	4.24	2.94	2.94	1.05	19.8	248.1	181.7	62.6	438.1	69.3	735.4	66.8	120.6	266.5	26.3	B. 7	3.1	5.7	6.0	19.0	11.6	•
4 - A	48.57	3.14	11.95	0	13.84	0.5	8.75	9.34	2.44	1.44	0.32	136	92.6	123.9	30	620.1	27.9	259.4	21.3	38.8	89.0	8.2	3.1	₹.1	1.9	0.0	S. S.		
F-4	48.79	17.71	13,47	0	13,83	0.18	7.46	8.43	2.46	1.7	0.38	179.4	84.1	123.1	28.5	831.6	28.1	297.2	19.6	45.6	105.0	4.6	3.3		2.2	4.0	7.1	3.2	
K-2A	53,33	3.03	12.93	•	15.29	0.18	2.8	3.96	2.77	2.75	0.95	11.6	137.1	167.7	72.5	961.8	62.1	647.9	53.3	110.7	231.0	23.1	7.8	0.0	n,	0.8	17.2	10.4	
-	54.48	3.51	14.22	•	11.63	0.19	4.27	6.94	2.91	1.35	0.8	47.4	106.1	132.1	28	826.5	29.6	303.8	24	44.7	95.3	9.6	3.6	1.4	2.3	n.o	6.7	5.2	
KC-11	53.82	3, 33	13.7	Э	13.41	0.16	3.93	4.49	4.13	2.26	0.74	27.1	242	165.9	41.3	503	47.9	504.2	47.4	81.2	182.6	17.7	6.2	2.1	0.4	0.7	12.3	7.8	
KC-88	. 31.6	₹	13.91	9	12.63	0.17	5.61	9.76	2.39	9.0	0.33	116.3	146.1	109.2	8.8	725.6	24.2	249.7	61	30.6	70.5	7.6	3.2	1.2	2.1	0.4	<b>S</b> .0	3.4	
KC-7	52.1	3.96	14.06	0	12.51	0.16	5.81	7.05	2.85	1.81	0.32	111.1	235	119.4	20.4	976	24.9	260.7	16.2	34.1	67.1	7.6	3.0	1.2	2.1	0.5	S	n. s.	
KC-6	52.91	3.29	15.03	0	13.47	0.13	3.62	5.18	3.83	1.89	0.65	25.2	168.6	162.7	44.8	1093.2	40.4	493.9	38.4	89.5	152.3	17.1	4.7	1.6	4.1	0.0	10.3	<b>၀.</b>	
	2018	T102	A1203	Fe203	F.0	OC E	<b>1</b> 90	0	N. 20	K20	P205	ž	S	<b>5</b>	8	'n	>	۲.	Ş	3	ů	es.	Eu	4	Ą X	רנ	Ì	£	,

Table 1 (Cont'd.)

DS-1	49.21	4.18	13.77	0	12.87	0.17	4.34	7.66	2.17	1.7	0.33	64.1	149	105.1	34.8	705.5	30.1	255.1	16.2	35.1	65.4	8.5	n n	1.2	2.6	0.4	6.5	4.1	59.3
BJ-PL	51.44	3.01	15.76	c	12.83	0.13	n. 10	7.54	3.67	1.62	0.5	8.3	31	129.8	30.6	934.2	32.3	370.9	27.3	67.0	143.4	12.0	4.1	1.6	3.2	0.5	8.5	5.9	9.6
BJ110	49.9	3.42	15.56	0	13.1	o. 13	5.23	6.09	3.8	2.26	0.49	47.5	64.1	139.5	7	896.9	33.1	348.9	27.4	57.4	128.2	e. ::	6.0	P) .	2.4	0 0	7.2	S.53	64.7
BJ-60	49.89	3.29	14.77	0	13.1	0.17	6.19	96.9	2.72	2.44	0.45	76	56.3	136	44.3	849.9	34.2	332.7	23.6	58.9	125.1	10.6	3.9	1.4	2.3	o.5	7.7	4.9	67.6
BJ-0	52.71	2.42	15.62	0	12.45	0.13	4.71	4.46	3.92	2.51	0.54	28.7	27.9	146.6	48.3	946.4	36.2	382	28.7	8.99	140.7	11.8	4.3	1.2	2.9	0.4	9.1	9.9	23.6
BJ-8F	51.35	n	16.04	0	12.14	0.16	5.56	5.66	3.29	2.22	0.37	32.7	11.6	162.1	35.6	722.1	36.5	373.1	32.1	70.9	146.1	12.0	4.3	1.4	٠. د.	o. s	8.8	6.2	21.6
N1-31	53.03	3.53	11.82	0	17.85	0.09	2.24	4.25	3.16	2.97	1.06	18.2	193	164.7	67.3	346.7	64.6	707.3	63	115.5	248.6	23.9	4.8	2.8	8.8	0.0	18.8	10.8	7.4
N1-24	51.75	n. 93	11.99	0	17.41	0.18	3.15	3.16	n.	2.24	1.07	8	193.7	181.3	50.6	422.1	94.9	720.2	99	113.7	247.2	24.8	8.0	4.8	6.1	0.7	18.1	11.3	11.3
	2018	1102	A1203	Fe203	Fe0	Š	<b>1</b> 90	0	Na20	K20	P205	ž	3	Zu Zu	£	ຸຮ	>	?r	9	•	ڻ	Š	Ec	2	Ą	ני	Ĭ	£	ີ່ບໍ່

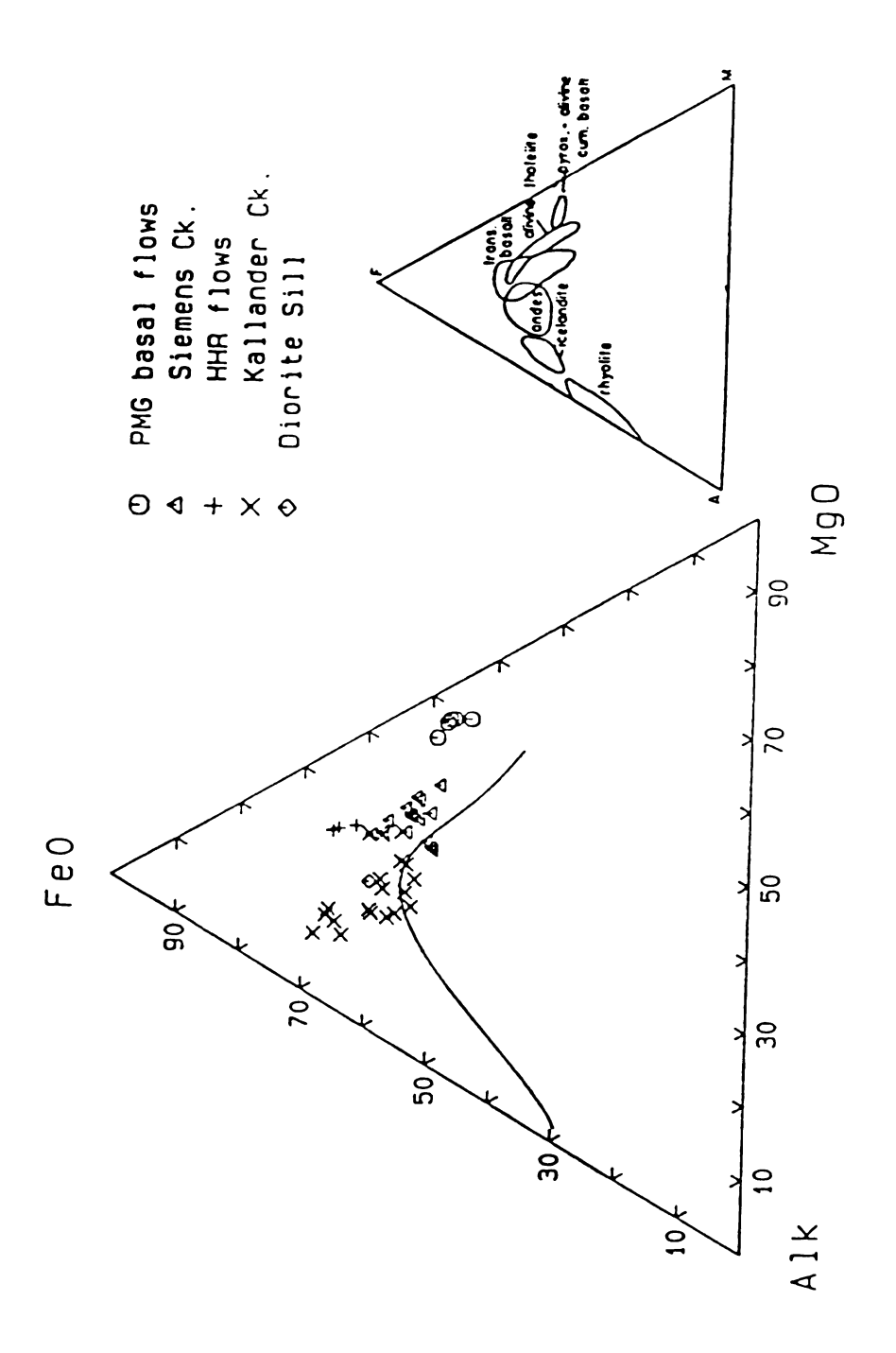


Figure 3 AFM Ternary Diagram

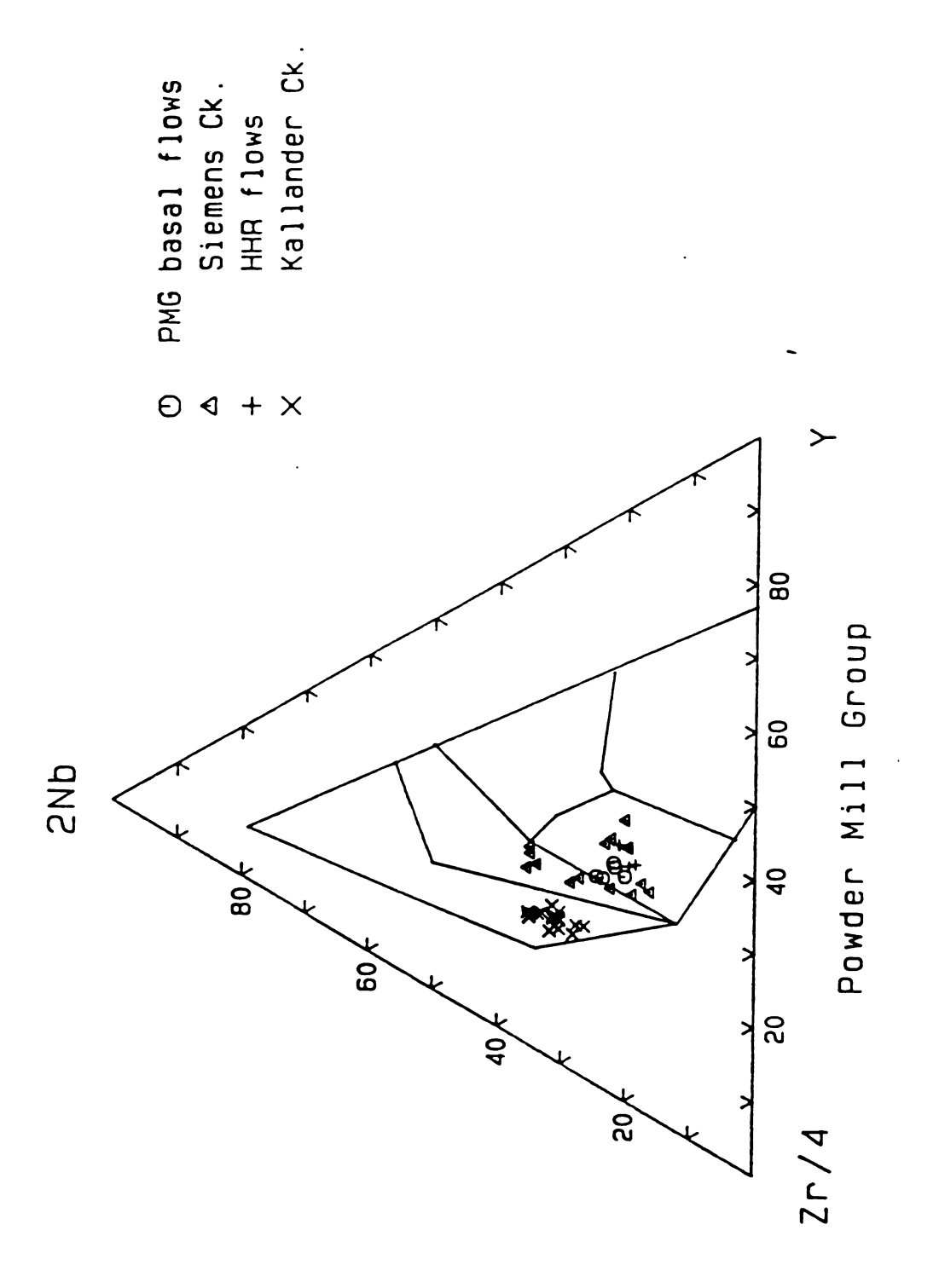


Figure 4 Nb-Zr-Y Diagram

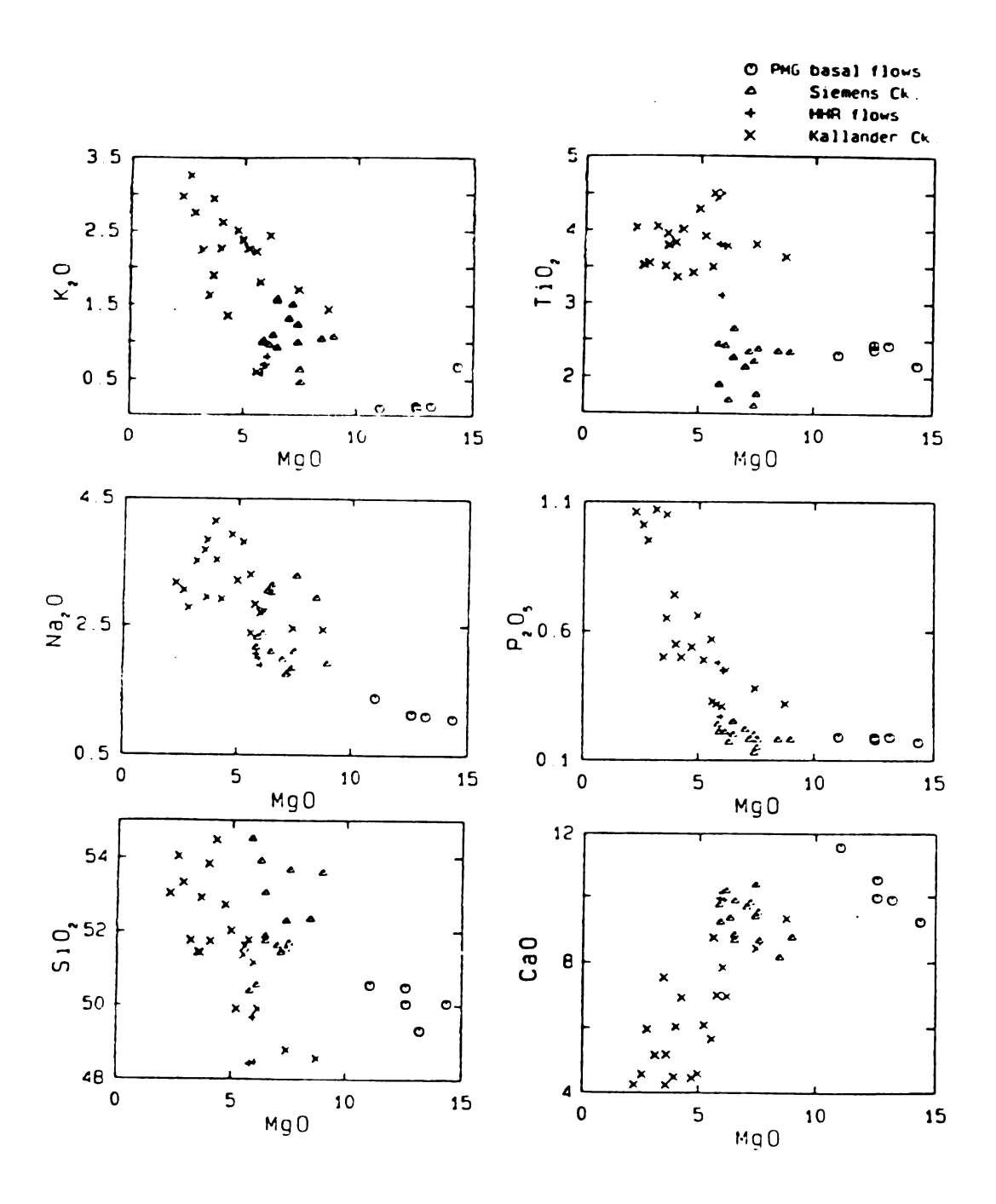


Figure 5 Variation Diagrams

observed by Wasuwanich of these elements is not present in the PMG lavas. The variation in the major elements in the PMG is continuous over their range. Variation diagrams (Figure 5) for selected major elements show their distribution against MgO. While there is some scatter in these diagrams they illustrate consistent trends in the data.

#### REE and TRACE ELEMENTS

Major elements, whose weight percents will total one hundred for each sample, are affected by the statistical problems of closure (Butler and Woronow, 1986). This is known as a constant sum effect that may hide or create trends in the major element data set.

REE and trace element behavior have been recognized as more sensitive to processes of magma generation and differentiation in basaltic systems (Yoder, 1976). Trace element decoupling from major elements contributes to this sensitivity; trace elements are not as intimately tied with the polymerization of the melt as are the major elements. This results in a greater response of the trace elements to changes during magmatic processes. Major element variation is far less than that of trace elements, indicating the greater sensitivity of the trace elements.

The use of trace element ratios rather than absolute values is important. It is assumed that trace elements behave in a predictable manner. A commonly used relationship is that of chondrite-normalized light rare earth elements (LREE) and the heavy rare earth elements (HREE). Partial melting of a chondrite source will enrich the liquid in the LREE relative to the HREE. Conversely, the original source will be depleted in the LREE relative to the HREE. Ratios make it possible to eliminate the influence of heterogeneous source concentrations, and examine relative trace

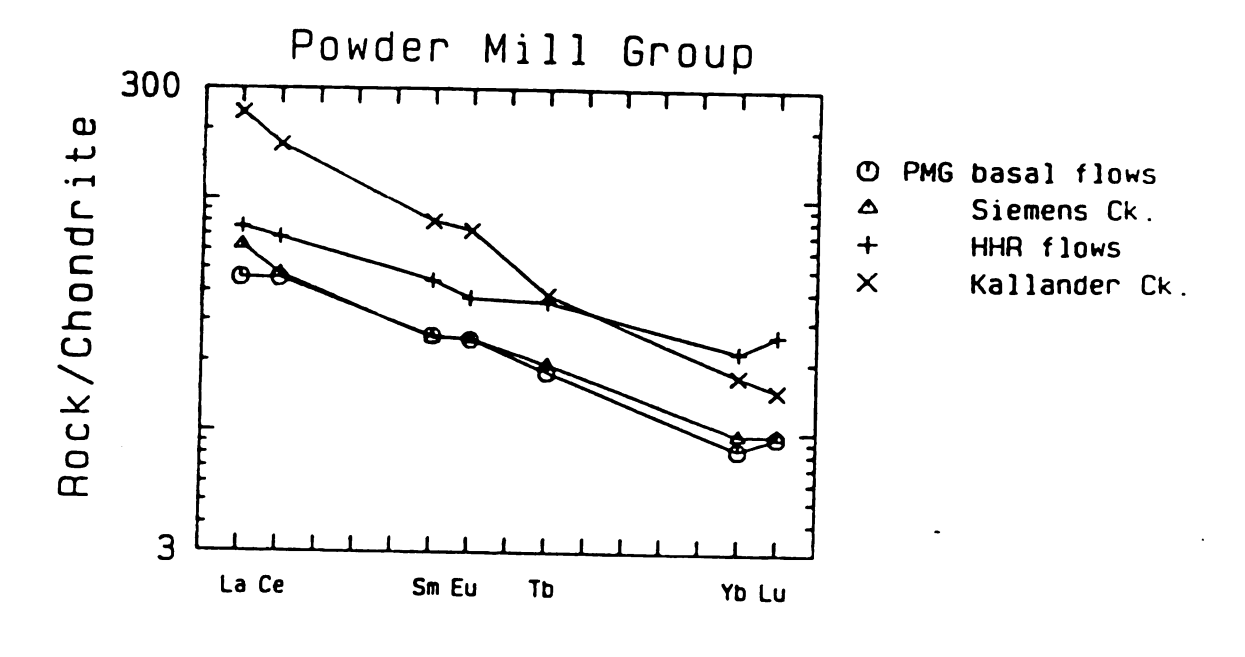
element behavior.

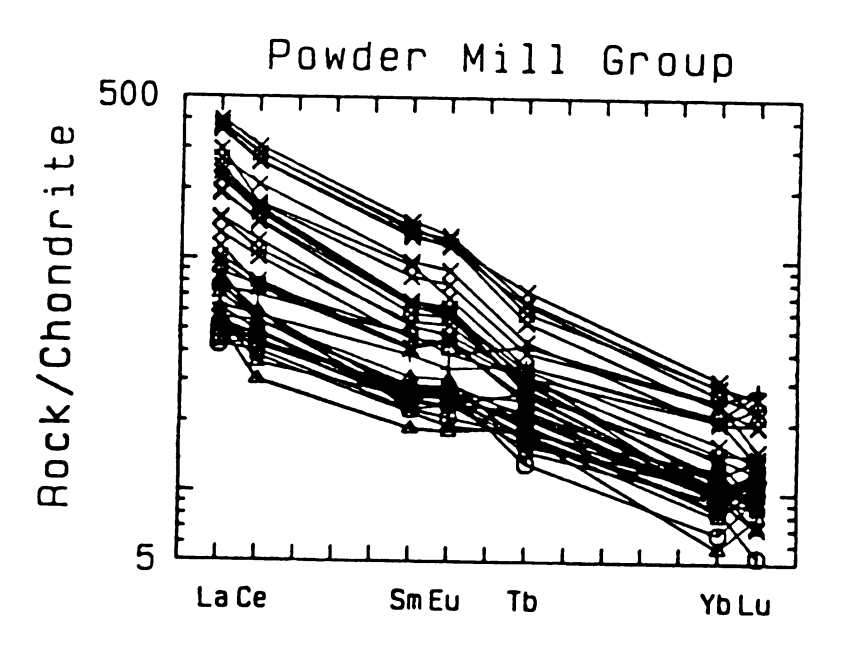
Plots of chondrite normalized REE data for the PMG are shown in Figure 6. Figure 6a includes the data for all of the rocks sampled in this study. A REE plot using averages for the respective groups is illustrated in Figure 6b. Basalts of the Siemens Creek Formation have slight LREE enriched trends. The variation in the relative abundances of the REE is limited to a relatively narrow range of about 40 to 90 times that of chondrite in the LREE. In Figure 6b the REE distribution in the basal flows of the Siemens Creek is almost identical to the rest of the Siemens Creek lavas. The Siemens Creek flows show no systematic variation in REE abundances with stratigraphic position. These rocks are not characterized by Eu anomalies. The Siemens Creek lavas have lower overall REE abundances than those of the Kallander Creek Formation.

The Kallander Creek lavas are more enriched in the REE than the Siemens Creek lavas and have slightly positive Eu anomalies in specimens with high overall REE abundances, as can be seen in Figure 6a. The La<sub>N</sub> (La normalized to chondrite) abundance ranges from 100 to 400 times greater than chondrite and are significantly enriched relative to the Siemens Creek lavas. The Kallander Creek lavas also have a slightly higher LREE enrichment ([La/Yb]<sub>N</sub>) than the Siemens Creek basalts.

The High HREE (HHR) flows are three samples from the Siemens Creek which are characterized by their REE distribution. They have a REE enrichment greater than that of the Siemens Creek but with a flatter trend of the REE than any of the other flows of the PMG as seen in Figure 6b.

Chondrite-normalized REE patterns (Figure 6a-6b) are consistent with lavas derived by partial melting and fractional crystallization. Partial melting of a source will cause variations in the ratio of one incompatible





(Chondrite values from Thompson et. al. 1982)
a) all PMG samples b) PMG averages

Figure 6 REE Chondrite-Normalized Plots

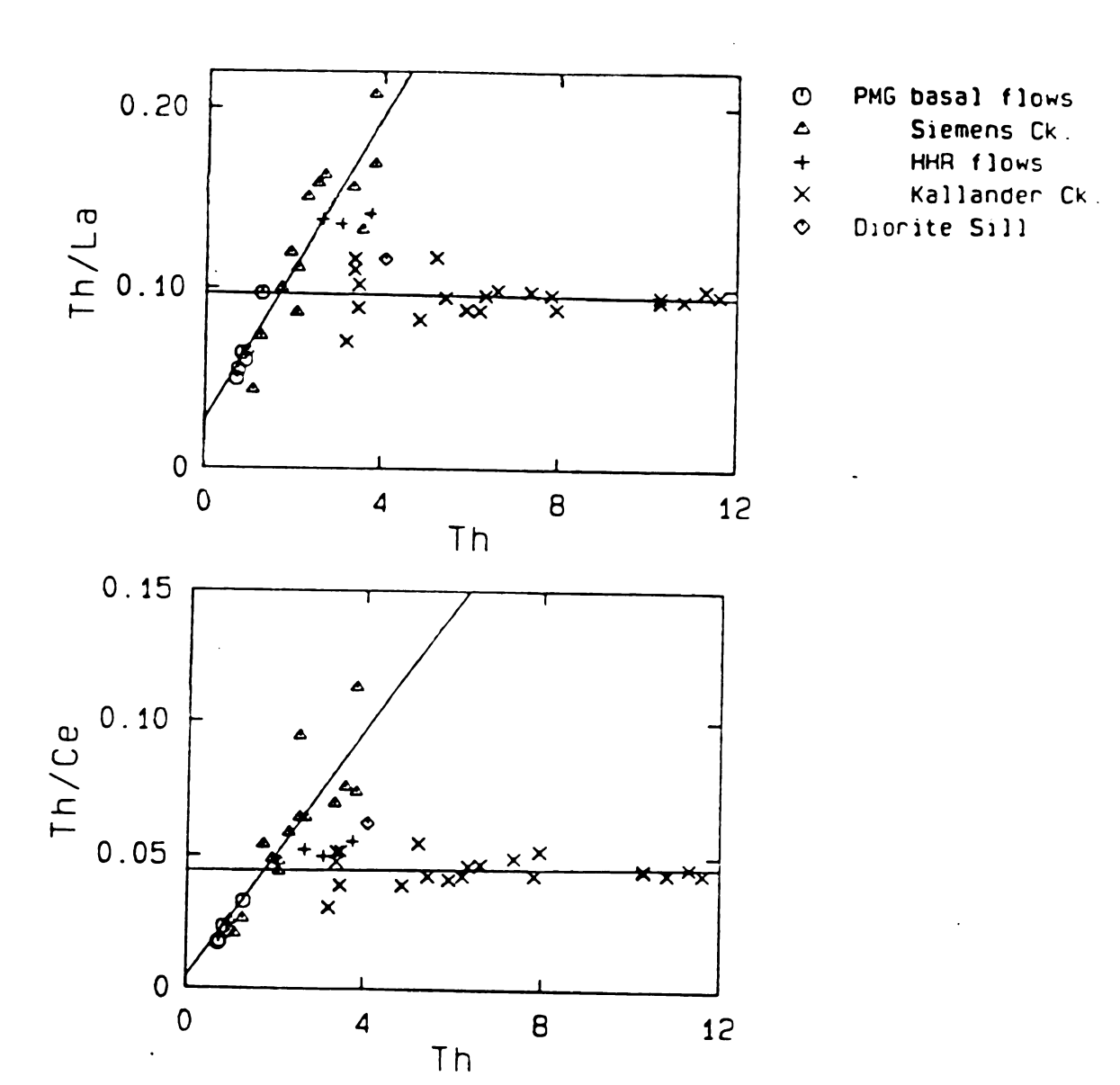
element with respect to another while effecting their absolute abundances little. The Siemens Creek lavas show little variation in the REE plot. However, the ratio variations of the Siemens Creek samples illustrated in the process identification diagrams (Figure 7a-7j) are relatively large.

Fractional crystallization processes cause the absolute abundances of the elements to change significantly while producing negligible variation in incompatible element ratios. The Kallander Creek lavas are more enriched in, and have a greater range of REE than the Siemens Creek lavas.

Variation of incompatible element ratios in the Kallander Creek rocks is small. The Kallander Creek lavas are more evolved derivatives of the PMG magmatic system.

"Spider" diagrams for the Lower Keweenawan lavas are shown in Figure 8. Figure 8a includes all of the Lower Keweenawan lavas. Figure 8b is a plot of the average of the Siemens Creek Formation and the average of the Kallander Creek Formation.

Figure 8b illustrates an enrichment in the Large Ion Lithophile (LIL) elements of the Siemens Creek average relative to those of the basal flows while the abundances of the High Field Strength (HFS) elements are nearly identical. This is consistent with the greater sensitivity of the LIL elements to varying degree of partial melting. As illustrated in the process identification diagrams the basal flows represent relatively large degrees of partial melting whereas the remaining Siemens Creek lavas are derivatives of smaller degree of partial melting. Conversely, the HFS elements are not very sensitive to varying degrees of partial melting and thus there is little difference between the distribution of these elements in the basal flows and the remainder of the Siemens Creek lavas. This supports the hypothesis that the Siemens Creek flows are the product of partial melting.



Process identification diagrams for: a) La, b) Ce, c) Sm, d) Eu, e) Tb, f) Yb, g) Lu, h) P<sub>2</sub>O<sub>5</sub>, i) Zr, j) Nb

Figure 7 Process Identification Diagrams

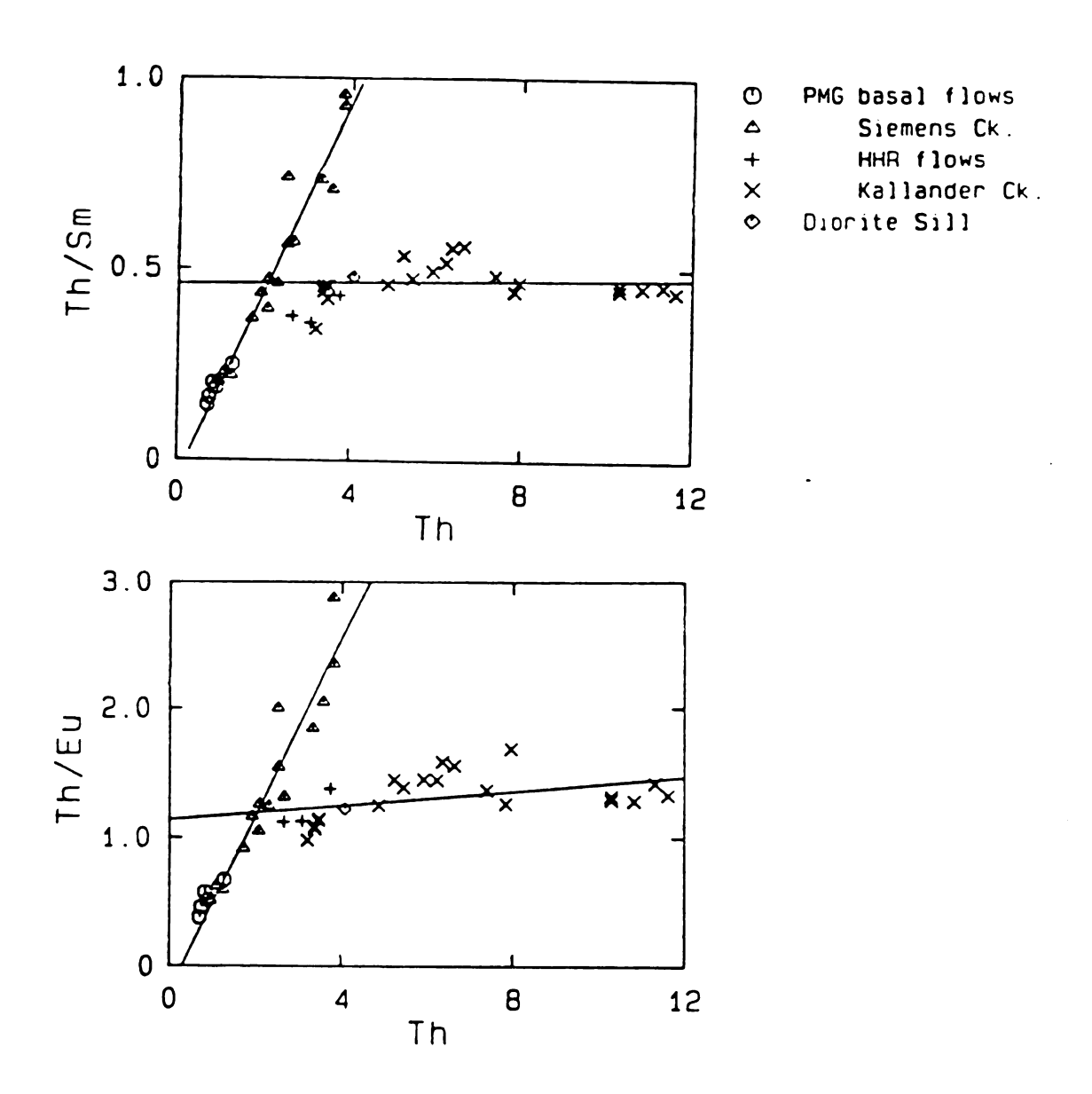


Figure 7 (Cont'd.)

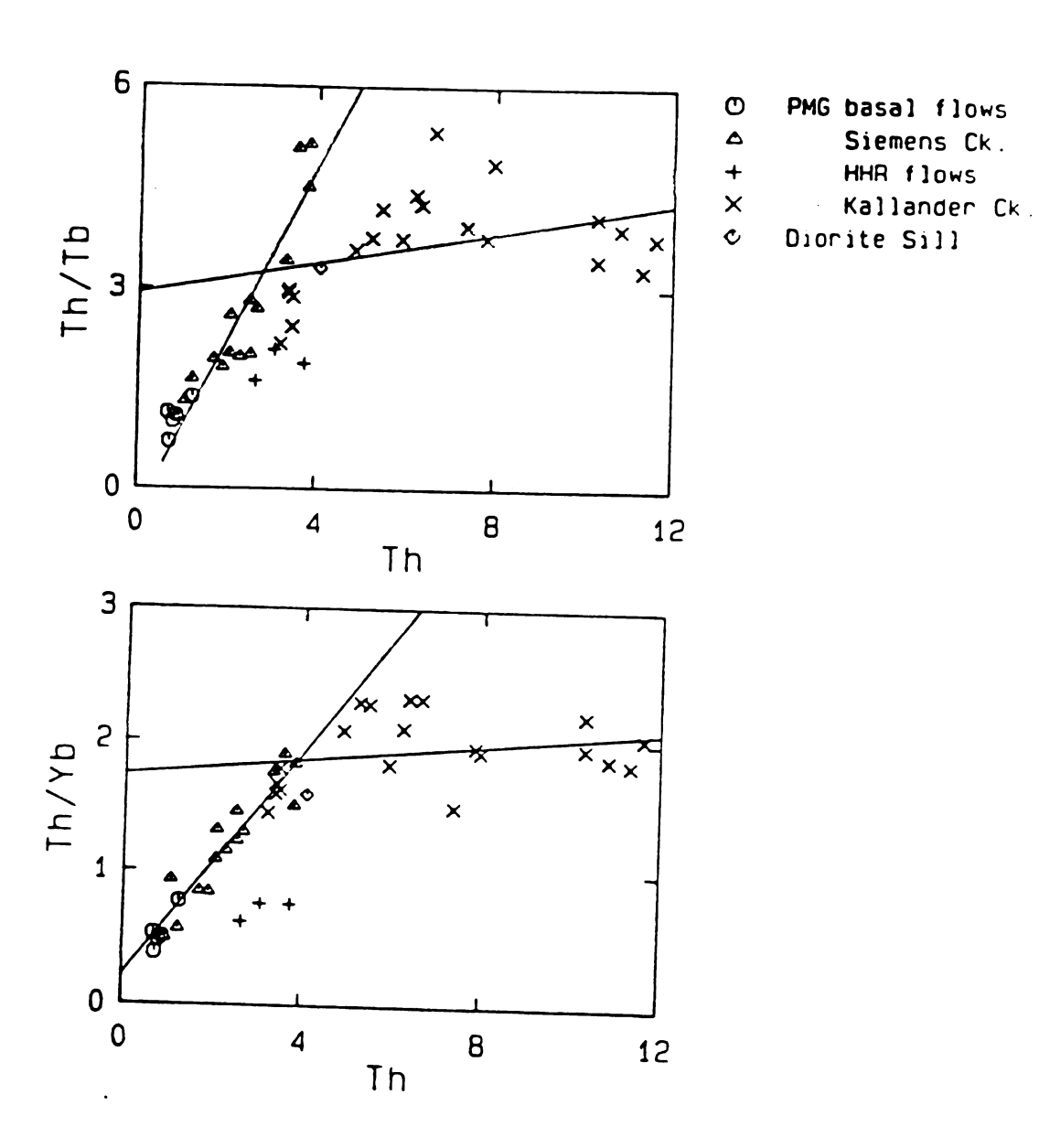


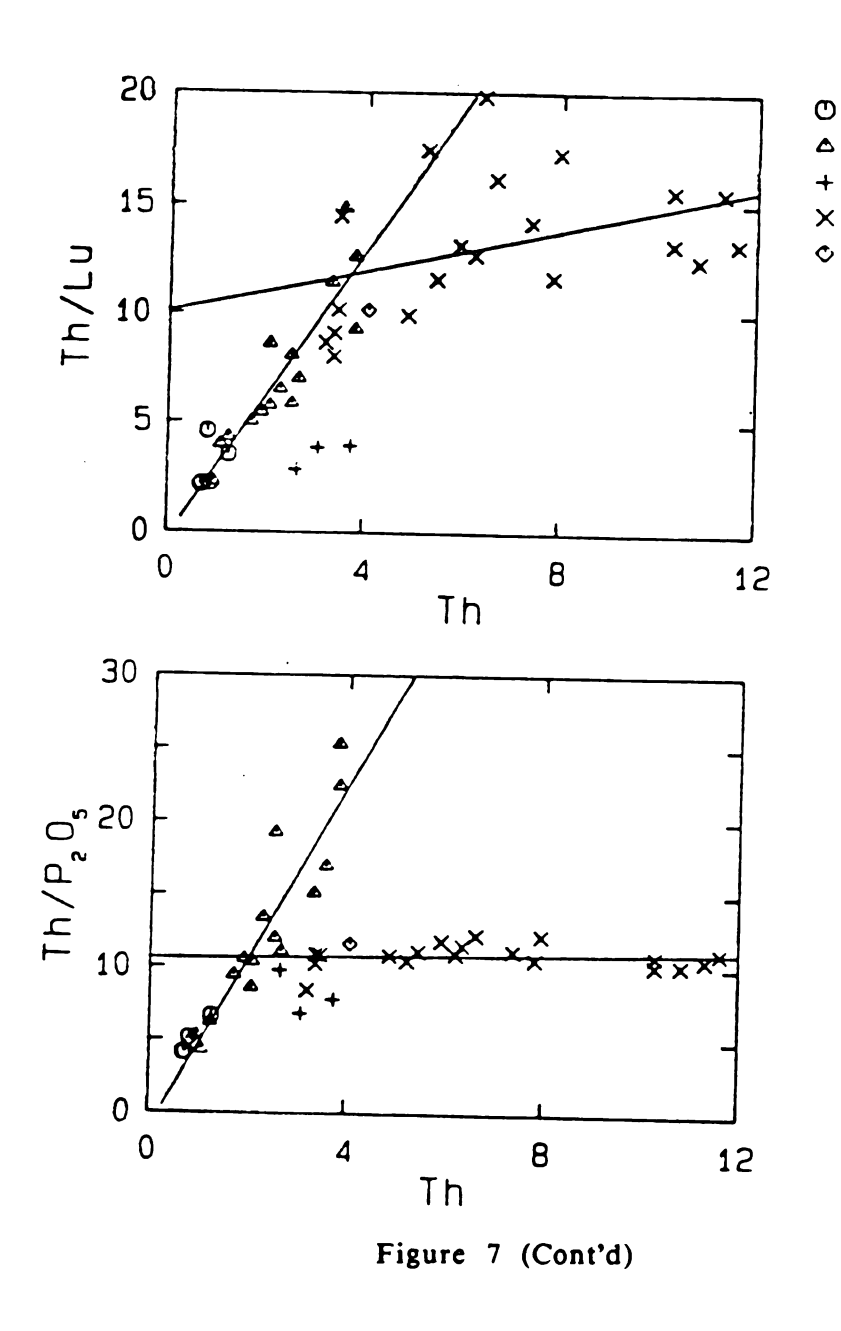
Figure 7 (Cont'd.)

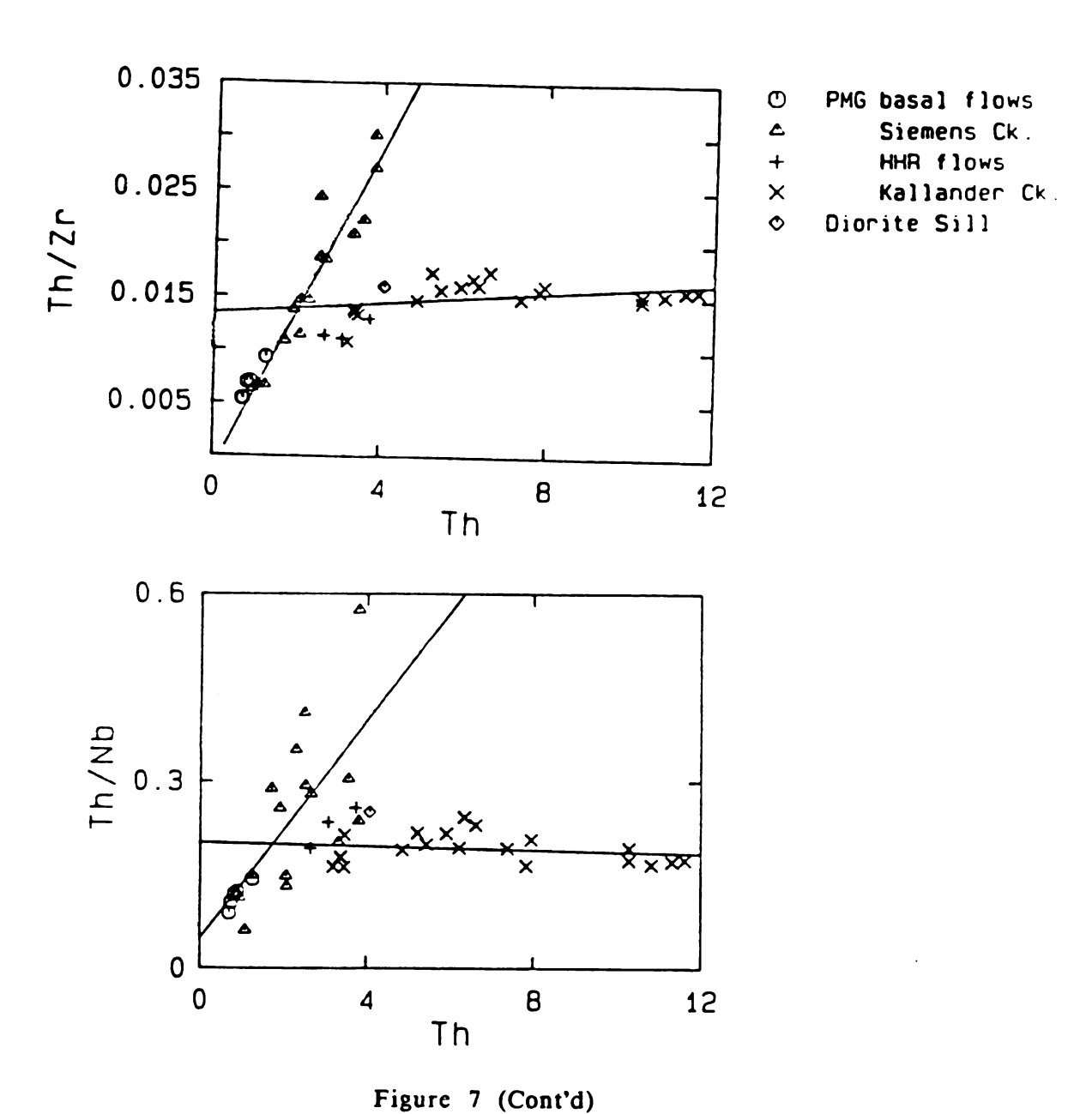
PMG basal flows

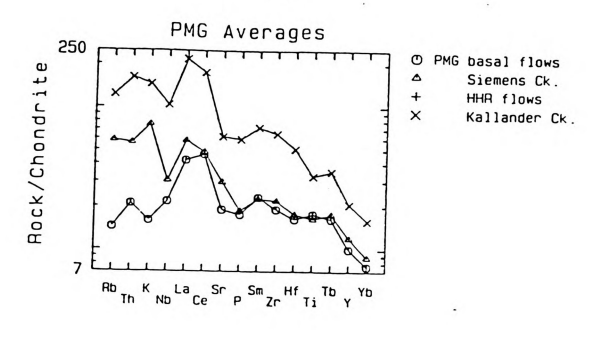
Diorite Sill

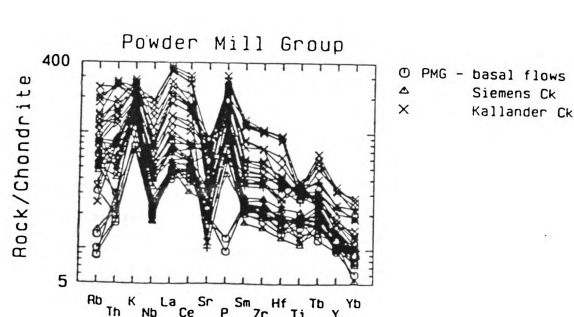
Siemens Ck. HHR flows

Kallander Ck.









(Chondrite values from Thompson et. al. 1982) a) all PMG samples b) PMG averages

Figure 8 "Spider" Plots

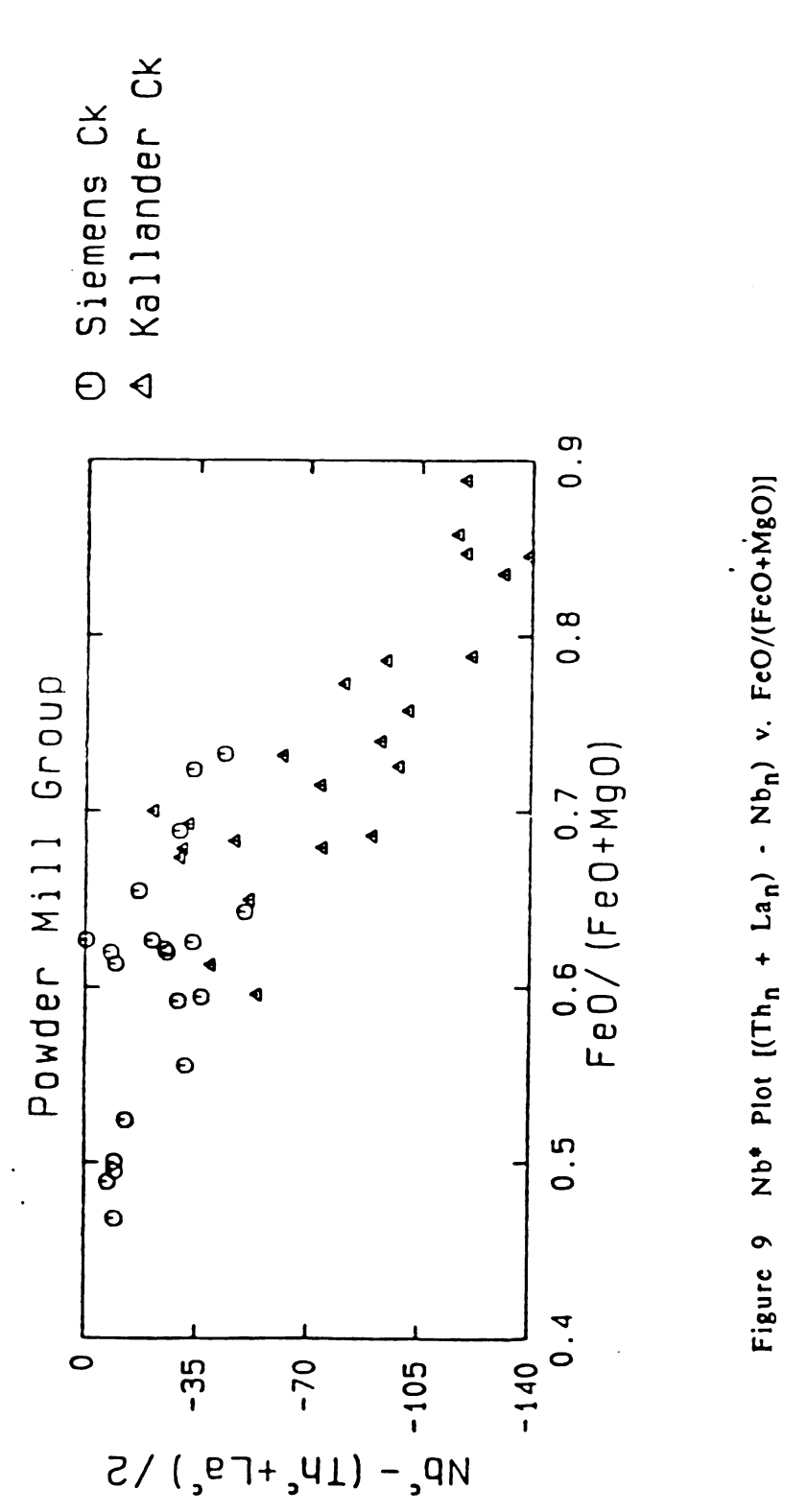
The Kallander Creek flows plot as an enriched trend in both the LIL and HFS elements. The behavior of the LIL elements and HFS elements is similar during fractional crystallization. Their behavior is illustrated in the process identification diagrams where the Kallander Creek lavas plot along a trend with little slope. Thus the Kallander Creek data plotted in the "spider" diagram is consistent with the hypothesis that the lavas were derived by fractional crystallization.

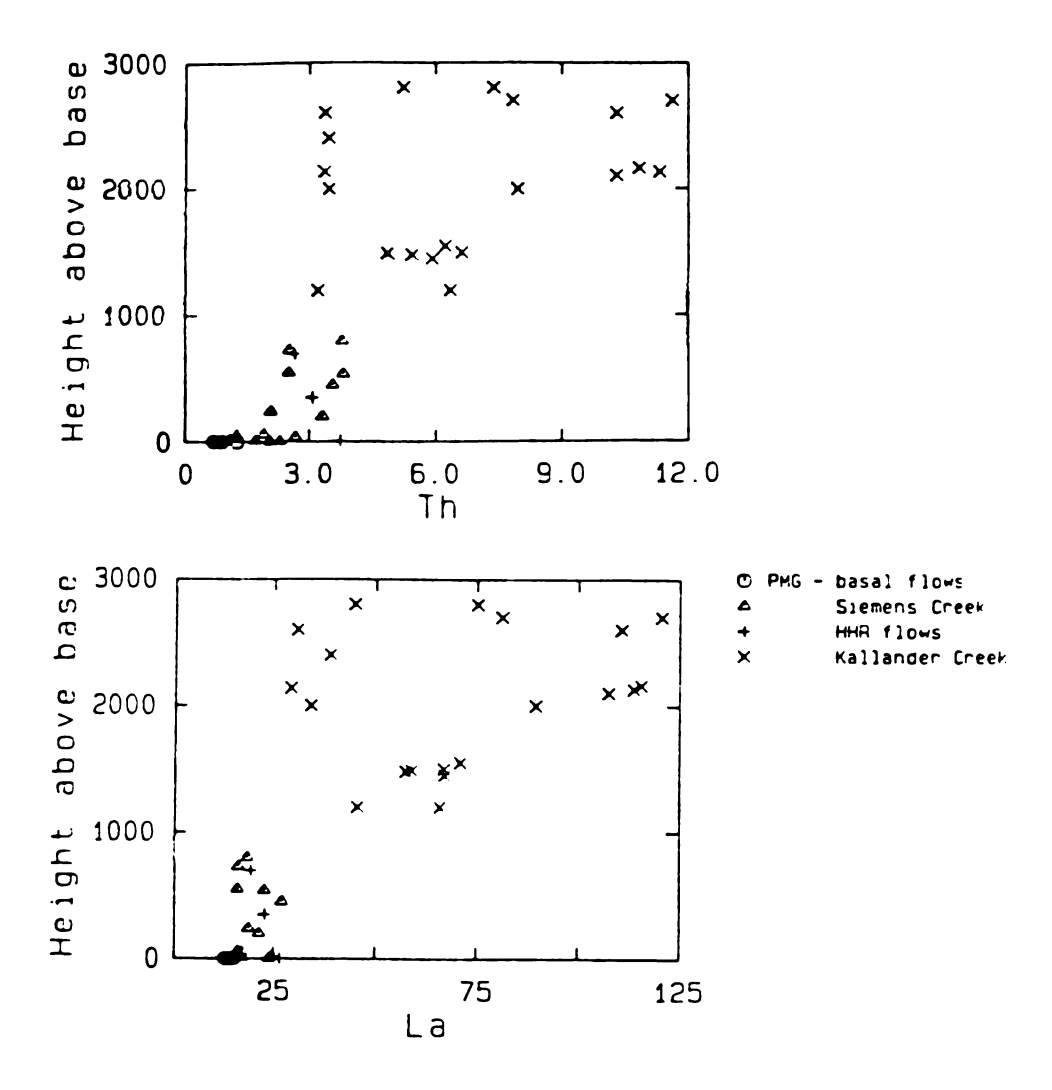
The Siemens Creek and Kallander Creek volcanics are depleted in Nb relative to the neighboring elements Th and La, as seen in Figure 8. This Nb depletion is illustrated in Figure 9 as a function of a differentiation index; FeO/(FeO + MgO). The Siemens Creek flows fall along a trend of low slope, while the Kallander Creek flows plot as a steeper trend.

Thompson et. al. (1982) have observed a similar trend in the Tertiary volcanics of Skye and Mull. They conclude that the Nb depletion is the result of crustal contamination by Nb depleted crustal material. Green and Pearson (1987) has documented high partitioning coefficients for Nb in Tirich phases during fractional crystallization.

These explanations are consistent with the trends observed in Figure 9. As the product of partial melting the Siemens Creek flows were erupted to the surface before they could be affected by fractioal crystallization or crustal contamination. The Kallander Creek lavas however, represent magma that ponded in the crust and underwent fractional crystallization. During this time the incorporation of Nb depleted crustal material and/or the fractionation of Ti-rich phases could account for an increasing Nb depletion.

Figure 10 illustrates the variation of Th and La with stratigraphic height. A general trend of enrichment with stratigraphic height is observed





Height is expressed in meters above basal contact.

Figure 10 Element Variation with Stratigraphic Height

in the diagrams. There is little change up section in the abundance of these elements the Siemens Creek, however in the Kallander Creek, the variation of these elements is much greater. These variations are also seen in the process identification diagrams where the Siemens Creek flows show little variation along the abscissa in the partial melting trend. Conversely the Kallander Creek flows show a broad variation along the abscissa. The Siemens Creek flows show no correlation of these elements with stratigraphic height. There is a trend in the Kallander Creek flows that shows a steady enrichment in Th and La with height above the base. These Figures illustrate a shift in the petrogenesis of the PMG lavas at about the 1000 meter level from partial melting to fractional crystallization.

The two populations of the PMG, the Siemens Creek lavas and the Kallander Creek lavas, are statistically different by the Student's T-test. Generally, the trace elements and REE of the Siemens Creek lavas are normally distributed. The Kallander Creek lavas are not normally distributed, but some within trace elements are log-normally distributed. Applying the T-test to the Siemens Creek data and log-corrected Kallander Creek data results in the rejection of the null hypothesis at the 95 confidence interval. The two populations are statistically different for the elements La, Ce, Sm, Eu, Tb, Yb, Lu, Zr, Nb, and Th.

### PETROGENETIC MODELING

Preliminary evaluation of the data was done using an approach developed by Treuil (1973) and Treuil and Joron (1975) as presented by Allegre and Minster (1978). This technique is based on hygromagmatophile elements (H elements) and magmatophile elements (M elements). H elements are the very highly incompatible elements whose bulk partitioning coefficients are negligible against values of 0.2-0.5, such as Th, and to a lesser extent La and Ce. The M elements are also incompatible but not to the same degree as the H elements. The M elements have bulk partitioning coefficients that are negligible against 1, such as Zr and the heavy REE.

During equilibrium partial melting, the H elements will be partitioned to the melt more effectively than the M elements. Assuming a constant source concentration, the change in the concentration of the H element (CH) will reflect the variation in the degree of partial melting (F) with,

$$C^{H} = \frac{1}{F} . \tag{1}$$

The concentrations of the H element and the M element in the melt increase as the degree of partial melting decreases, but the H element concentration increases at a faster rate. In a plot of the ratio of an H element and an M element over the range of the H element (referred to as a process identification diagram), lavas that are generated by partial melting will plot as a line with a positive slope.

For lavas generated by fractional crystallization, the H element and

the M element will behave similarly. As the melt composition changes during fractionation, the rate of change in the two elements will be nearly identical. When plotted on a process identification diagram the data will plot as a line with slope near zero.

The process identification diagrams for the PMG can be seen in Figure 7. The has been selected as the H element for these plots. Clague and Frey (1982) determined The to be the most incompatible element in their examination of the Honolulu Volcanics. The is highly correlated with other incompatible trace elements and has the widest range of values. They also note that plots of trace element abundances against The produce intercepts greater than zero. Clague and Frey (1982) interpret this to indicate either varying trace element abundances in the source or that the trace elements have a slightly higher bulk-solid/melt partition coefficient than Th. In the PMG, The is highly correlated with the other trace elements and has positive intercept values. The also has a greater abundance range than La or Ce; The varies by a factor of about 5.5, La by 2.1, and Ce by 2.0.

The M elements used in the process identification diagrams are La, Ce, Sm, Eu, Tb, Yb, Lu, Zr, P<sub>2</sub>O<sub>5</sub>, and Nb.

A consistent pattern is exhibited in each of the plots (Figures 7a-7j). The Siemens Creek lavas plot in a trend with positive slope, consistent with partial melting. The lavas that have the lowest ratio values represent the largest degree of partial melting. The lavas which exhibit the largest ratios represent the smallest degree of partial melting.

The Kallander Creek lavas plot as a trend with slopes that approach zero, consistent with fractional crystallization. The samples with the lowest Th values in this trend represent the least fractionated derivatives while the highest Th values represent the most fractionated.

There is no correlation of stratigraphy with the degree of partial melting or fractional crystallization in these diagrams. This may be the result of variable transport times to the surface or tapping of different levels in the magma chamber. The lack of a stratigraphic correlation is not considered a significant problem in this study.

Three Siemens Creek samples are plotted as transitional lavas because they do not appear to be associated with either trend. They have chondrite-normalized plots that are distinct from those of the other two groups (Figure 6). It appears that these samples represent lavas erupted as the dominant magma generating process shifted from partial melting to fractional crystallization.

A diorite sill described by Hubbard (1975) as a stratigraphic marker between the Siemens Creek and the Kallander Creek is also plotted. From Figure 7, the sill appears to be a geochemical marker as well as a stratigraphic marker.

Allegre and Minster (1978) have developed quantitative techniques for constraining the parameters of trace element behavior during partial melting. They propose an inverse method to test for equilibrium batch partial melting. The method derives the source ratio of two elements from the Y-intercept values of the process identification diagrams. In a successful application of this technique, Clague and Frey (1982) were able to constrain source concentration and degree of partial melting for the Honolulu Volcanics. Following their reasoning, less successful results were obtained from estimates of source composition for the PMG lavas. Calculations are based on the composition of sample AP-15, assumed to represent the highest degree of partial melting, gave intercept values (Table 2) which are inconsistent with current mantle models and trace element

Table 2 Process Identification Diagram Intercept Calculations

Element (i)	В	Α	r <sup>2</sup>
La	0.0265	0.0422	0.910185
Се	0.0024	0.0237	0.909744
Sm	-0.0319	0.2403	0.974013
Eu	-0.1126	0.6559	0.959944
Tb	-0.1549	1.2133	0.946861
Yb	0.1648	0.4421	0.951767
Lu	-0.0425	3.1696	0.916820
Zr	-0.0020	0.0071	0.958436
Nb	0.0407	0.0894	0.730297
$P_2O_5$	-0.4915	5.6384	0.934190

Values for line y=Ax+B generated least-squares best fit regression of partial melt data, where A is the slope and B is the intercept. Element (i) is the element in the process identification diagram, Th/i vs. Th.

behavior.

The process identification diagrams show the Kallander Creek data is consistent with fractional crystallization. The equation describing the change in the liquid composition during simple fractional crystallization is given by Cox et. al. (1979) as

$$\begin{array}{c} C_1 \\ \cdots \\ C_2 \end{array} = F^{(D-1)} , \qquad (2)$$

where

C<sub>1</sub> = the concentration of an element in the residual liquid; C<sub>0</sub> = the concentration of an element in the original liquid; F = weight proportion of residual liquid;

D = the bulk partitioning coefficient.

For elements with bulk distribution coefficients that are very small,  $C_1/C_0$ will vary as a function of 1/F. Because H elements and M elements have bulk distribution coefficients that are negligible against 1, their  $C_1/C_0$ variations will be nearly identical. The ratio of an H element and an M element will remain constant over the H element range. This is illustrated by the Kallander Creek lavas in the process identification diagrams.

Methods for quantifying the behavior of the trace elements during fractional crystallization have been developed for a variety of circumstances. The influence of disequilibrium fractional crystallization, an escaping fluid phase, liquids trapped in the cumulate, and fractionation in a convecting magma chamber are presented quantitatively by Allegre and Minster (1978). O'Hara and Mathews (1981) present a model for an advancing magma which is periodically tapped, periodically replenished, and continuously fractionating. Huppert and Sparks (1984) have described the effects of double diffusion-convection in crystal fractionation. models are examples of variations from the simple fractionation model

(equation 2).

There are no techniques for objectively limiting the variables, as with the inverse method for partial melting suites. It is difficult to constrain the degree of fractionation, variability of the partitioning coefficients, or the composition of the fractionating phases. These parameters may be constrained by experimental methods and detailed compositional analysis of the matrix and phenocrysts. The fractional crystallization models give non-unique solutions, and only suggest a particular model is consistent with the data set.

Minster et. al. (1977) have applied the inverse technique to fractional crystallization modeling. This method involves solving simultaneous equations by matrix analysis to provide a best fit to the observed data. It requires a more detailed data set than that available. It also requires a priori constraints in the form of a preferred model. Therefore it cannot be applied to the Kallander Creek lavas at this time.

Modeling of the major elements in the fractionation trend is useful for constraining the amount of fractional crystallization indicated in the process identification diagrams. The results of multiple linear regression analysis, using phenocryst data (Wilband, pers. comm) from the most primitive Keweenawan diabase dikes of Michigan, as seen in Table 3. Sample K-4 is used as a parent liquid from which the most evolved lava, K-7, can be produced by the fractionation of olivine, pyroxene, plagioclase, and ilmenite at a ratio of 0.16:0.43:0.36:0.05 respectively for the PS-12 data and 0.18:0.44:0.31:0.07 respectively for the JW-4 data. At these ratios 40 to 45 percent of K-4 is fractionated.

Modeling of the fractional crystallization trend following the method of Cox (1979) gives a reasonable fit assuming sample K-4 as the parent

Table 3 Multiple Linear Regression Analysis Calculations

	Independent variable	Coefficient	Std. error	
A)	CONSTANT	-0.06355	0.138191	
	<b>K-</b> 7	0.602252	0.017681	
	OLIVINE	0.066495	0.011133	
	PLAGIOCLASE	0.175261	0.013965	
	AUGITE	0.145320	0.018504	
	ILMENITE	0.024518	0.006818	
	R-square = 0.9995			
	Standard error = 0.316769			
	***********			
B)	CONSTANT	0.006131	0.082775	
	<b>K-7</b>	0.556211	0.011853	
	OLIVINE	0.079390	0.006744	
	PLAGIOCLASE	0.199775	0.008939	
	AUGITE	0.139003	0.009933	
	ILMENITE	0.025550	0.004132	
	R-square = 0.9998			
	Standard error = 0.190449			

The parent liquid (dependant variable) is sample K-4. A) Calculations based on phenocryst data from diabase dike PS-12. B) Calculations based on phenocryst data from diabse dike JW-4.

magma and fractionating olivine, pyroxene, and plagioclase in a ratio of 0.30:0.20:0.50, respectively in 5 weight percent increments. With 59 percent of the original liquid remaining, the model produced a liquid composition similar to the most evolved sample, K-7. An alternative model, using the same crystallizing phases, is produced by fractionating at a ratio of 0.35:0.15:0.50 in 5 weight percent intervals. Neither of these results correspond to the regression analysis. This is interpreted as evidence that either the phenocryst data from the dikes are not indicative of the phases that fractionated from the magma, or that the model of Cox (1979) is too simple to account for the variations seen in the PMG rocks.

Wallrock assimilation in an ascending magma can result in elemental variations unrelated to the processes of generation. Thompson et. al. (1982) were able to quantify the effects of crustal contamination on the Paleocene plateau lavas of Skye and Mull in Scotland. Both the lavas and the Archean Lewisian continental crust have well characterized isotope and trace element abundances. This has permitted the effects of the continental crust on the intruding lavas to be recognized. Data for the crustal rocks intruded by the Lower Keweenawan lavas, as well as the lavas themselves, are not adequate to estimate the effects of contamination. Thus the effects of wallrock assimilation on the PMG lavas has not been evaluated, but cannot be eliminated as a possible source for some degree of the observed elemental variation.

#### RESULTS

The basal flows of the Siemens Creek Formation are chemically and petrographically distinct from all later Keweenawan eruptives. Their major and trace element chemistry is the most primitive of the Lower Keweenawan lavas with the highest compatible element concentrations and lowest incompatible element concentrations. The abundance and size of phenocrysts in these flows are unusual for Keweenawan flows in Michigan. The pyroxene phenocrysts may be high pressures phases on the liquidus in the upper mantle. However, the occurance of the pyroxene with olivine and plagioclase phenocrysts, indicate the magma resided under conditions in which the phenocrysts were on the liquidus. The texture may also have been the result of the mixing of two liquids formed at different depths; A deep melt in which pyroxene is on the liquidus, and a shallower melt in which olivine and plagioclase are on the liquidus.

The rapid eruption of these initial lavas to the surface preserved the textures of the magma. The later Siemens Creek lavas ascended through the crust at a rate rapid enough to not allow large pyroxene phenocrysts to form

Variation of the Siemens Creek trace element and REE ratios in process identification diagrams is along a trend of positive slope, indicative of melts generated by partial melting. The basal flows have the lowest ratio values and represent the largest degree of partial melting. Later lavas that plot with higher ratios are the product of smaller degrees of partial melting but there is no clear correlation between degree of partial

melting and stratigraphy. Quantitative modeling of the partial melt suite is not successful but does not invalidate the findings from the process identification diagrams.

Trace element and REE ratio variation of the Kallander Creek lavas in the process identification diagrams is along a trend with slope near zero.

This is indicative of magmas generated by fractional crystallization. While the ratio in the diagrams remains constant, the lavas with the highest incompatible element concentration represent the most evolved.

The Kallander Creek lavas are generally more evolved with higher incompatible element concentrations and lower compatible element concentrations. Petrographically, the lavas have a consistently lower percentage of mafic minerals than the Siemens Creek lavas. There is a correlation of increasing proportion of plagioclase with greater degrees of fractionation. As the ponded magma fractionated, the buoyant plagioclase became an increasingly dominant phase in the erupted liquid. The most evolved lavas are the "turkey track" lavas which reflect a plagioclase dominated magmatic liquid; the result of fractional crystallization and density stratification.

Modeling of the Kallander Creek rocks using major elements and a simple fractionation model reproduced the fractional crystallization trend. Similar results were achieved with multiple linear regression using phenocryst data from the most primitive Keweenawan diabase dikes. This supports the evidence from the process identification diagrams that the Kallander Creek lavas were derived by fractional crystallization.

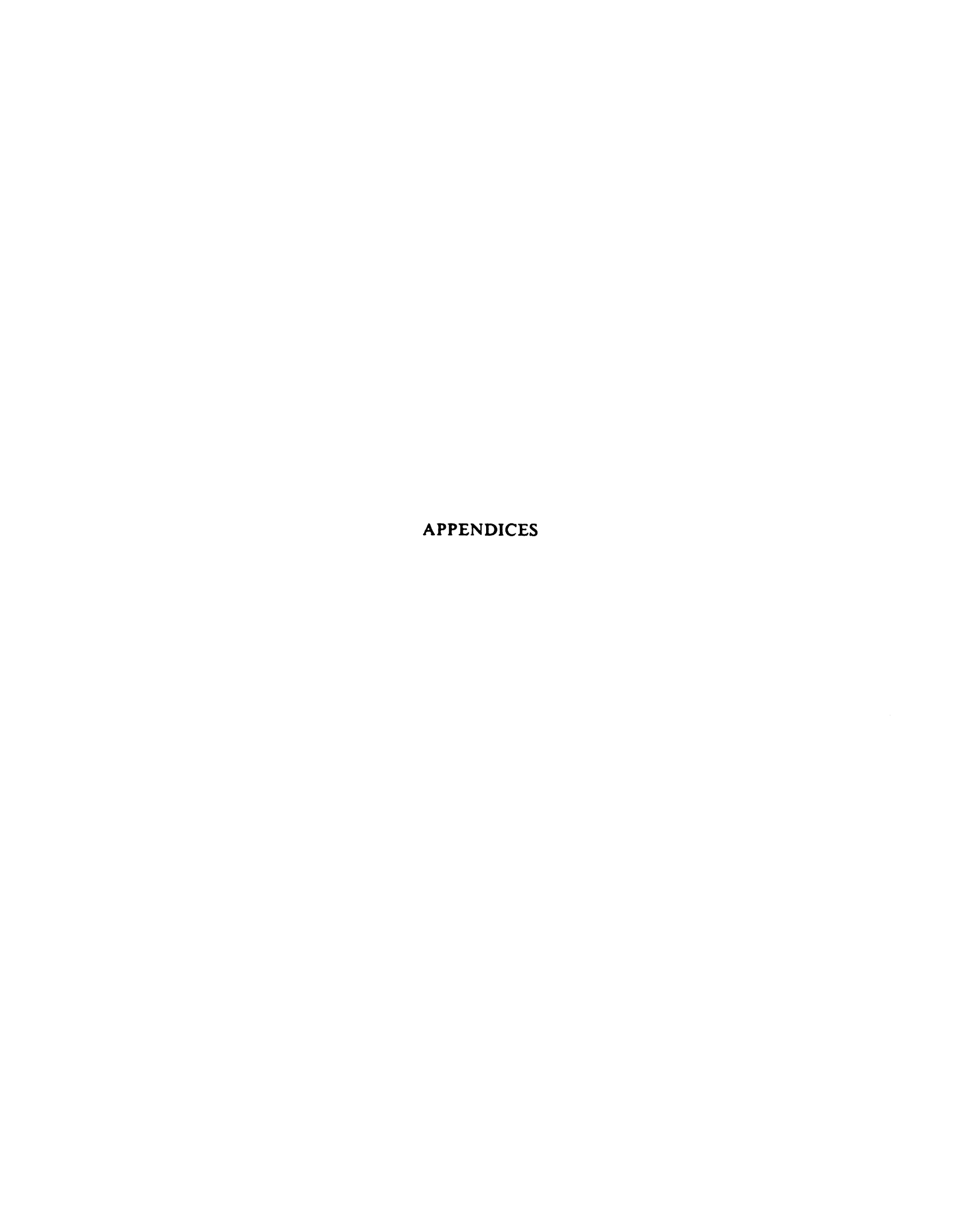
The lack of a Eu anomaly in the REE diagrams in all but the most evolved rocks of the PMG is not considered evidence against the fractionation of plagioclase from the melt. A similar pattern of Eu

distribution is observed in other continental flood basalts. Modeling of Eu distribution for a tholeiitic liquid (Miller, 1986) indicates that Eu concentration is not greatly affected by plagioclase fractionation.

The observed Nb depletion is interpreted to be the result of some combination of contamination by a Nb depleted crust or the removal of Nb from the magma by fractionation of Ti-rich phases. This supports the hypothesis for the petrogenesis of the PMG lavas. The more evolved Kallander Creek flows showing a greater degree of contamination due to ponding and fractionation in the crust.

The variation of Th and La with stratigraphic height also illustrate the development of the magmatic system. The clustering of the values in the Siemens Creek Formation and the greater spread of values in the Kallander Creek Formation as seen in Figure 10 illustrates a major shift in the petrogenesis of the magmas.

The lavas of the PMG are interpreted to represent changing magmatic processes during the MCR. About 1.2 Ga the tensional tectonic forces of the MCR caused crustal thinning and fracturing. Magmas generated by partial melting of the upper mantle were erupted to the surface through a developing fracture system. As the volume of this "plumbing" system became more extensive, magmas derived by partial melting could not reach the surface and ponded in the crust. The ponded magma fractionally crystallized while periodically erupting to the surface, becoming progressively more evolved until volcanism ceased locally. However, other centers volcanism continued to develop and wane in other areas along the rift.



### APPENDIX A: ANALYTICAL METHODS

Bulk rock chemistry was determined using X-ray fluorescence and Instrumental Neutron Activation Analysis (INAA) for 60 samples. Samples were slabbed, trimmed of any weathered rind and secondary mineralization, and ground to a homogeneous powder (200 mesh). Powdered samples were dried in an evacuated oven at 50 C for 24 hours to remove nonstructural water.

For X-ray fluorescence analysis two types of sample preparation were used. Glass wafers were made using 1.0000 gram of dried sample, 9.0000 grams of lithium tetraborate, and .1600 grams of ammonium nitrate. This mixture was liquified by firing for 30 minutes at about 1100 C. The mixture was poured into a mold and slowly cooled. The glass wafers were used to analyze for Si, Al, Fe, Mg, Ca, Na, K, Ti, P, and Mn.

Analysis for trace elements Cr, Ni, Cu, Zn, Rb, Sr, Y, Zr, Nb, and La by X-ray fluorescence were done using pressed powder pellets.

INAA was conducted using 1.00000 gram powdered samples in sealed polyvinyl vials. Samples were irradiated for about 18 hours over a 3 day period. Elements analyzed were La, Ce, Sm, Eu, Tb, Yb, Lu, Hf, Th, and Cr.

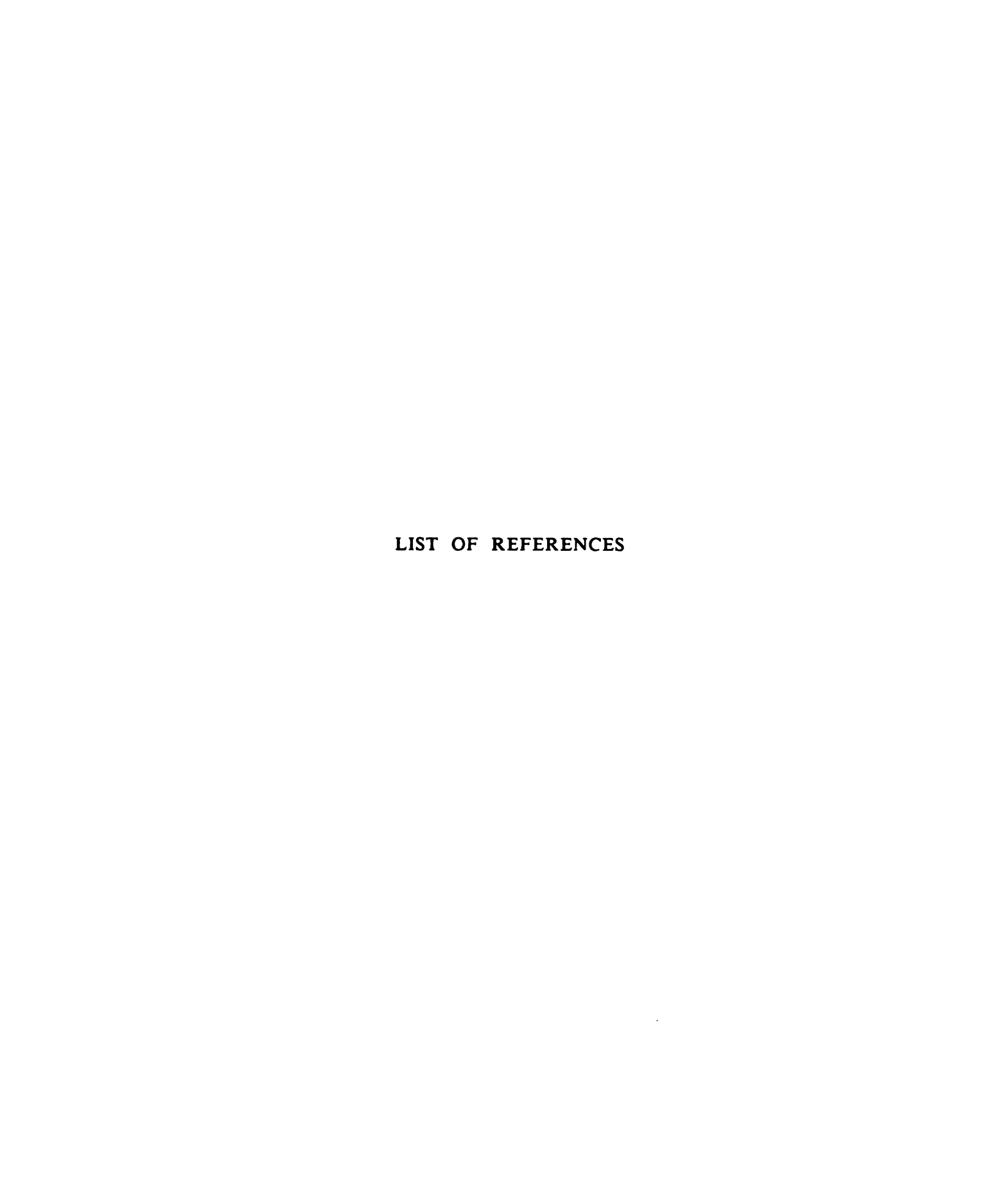
# APPENDIX B: INSTRUMENTATION

## X-ray Fluorescence:

- -Rigaku X-ray Fluorescence Spectrometer
- -Rh X-ray tube
- -Flow-proportional counter with P-10 gas (90 % argon, 10 % methane)
- -LIF, ADP, and PET analyzing crystals
- -VAX 1170 computer and software for concentration calculations

## INAA:

- -Triga Mark I reactor
- -Canberra GeLi detector (lithium drifted germanium crystal held at cryogenic temperatures by liquid nitrogen)
- -Canberra Series 35 Multichannel analyzer
- -associated amplification electronics
- -IBM-XT interface and software



### LIST OF REFERENCES

- Allegre, C.J. and Minster, J.F., 1978. Quantitative models of trace element behavior in magmatic processes. Earth and Planetary Science Letters, 38, 1-25.
- Books, K.G., 1972. Paleomagnetism of some Lake Superior Keweenawan lava flows in the Lake Superior area. United States Geologic Survey Professional Paper, 760, 42.
- Butler, J.C. and Woronow, A., 1986. Discrimination among tectonic settings using trace element abundances of basalts. Journal of Geophysical Research, 91, no. B10, 10,289-10,300.
- Clague, D.A. and Frey, F.A., 1982. Petrology and trace element geochemistry of the Honolulu Volcanics, Oahu: Implications for the oceanic mantle below Hawaii. Journal of Petrology, 23, pt. 3, 447-504.
- Cox, K.G., Bell, J.D., and Pankhurst, R.J., 1979. The interpretation of igneous rocks. George Allen & Unwin Limited, London. 450 p.
- Gordon, M.B. and Hempton, M.R., 1986. Collision-induced rifting: The Grenville orogeny and the Keweenawan rift of North America. Tectonophysics, 127, 1-25.
- Green, J.C., 1983. Geologic and geochemical evidence for the nature and development of the Middle Proterozoic (Keweenawan) Midcontinent rift of North America. In: Processes of continental rifting. P. Morgan and B.H. Baker (editors). Tectonophysics, 94, 413-437.
- Green, J.C., 1982. Geology of Keweenawan extrusive rocks. In: Geology and tectonics of the Lake Superior Basin. Wold, R.J. and Hinze W.J. (editors). Geologic Society of America Memoir 156, 280 p.
- Green, T.H. and Pearson N.J. 1987. An experimental study of Nb and Ta partitioning between Ti-rich minerals and silicate liquids at high pressures and temperatures. Geochimica et Cosmocimica Acta, 51, 55-62.
- Hubbard, H.A., 1975. Lower Keweenawan volcanic rocks of Michigan and Wisconsin. United States Geologic Survey Journal Research, 3, 529-541.
- Huppert, H.E. and Sparks, R.S.J., 1984. Double-diffusion convection due to crystallization in magmas. Annual Review of Earth and Planetary Sciences, 12, 11-37.

- Irving, R.D., 1883. The copper-bearing rocks of Lake Superior. United States Geologic Survey Monograph, 5, 464 p.
- Irving, T.N. and Barager, W.R.A., 1971. A guide to the chemical classification of the common volcanic rocks. Canadian Journal of Earth Sciences, 8, 523-548.
- King, E.R., 1975. A typical cross section based on magnetic data of Lower and Middle Keweenawan volcanic rocks, Ironwood area, Michigan. United States Geologic Survey Journal Research, 3, 543-546.
- Langmuir, C.H., Vocke, R.D., Hanson, G.N., and Hart, S.R., 1978. A general mixing equation with applications to Icelandic basalts. Earth and Planetary Science Letters, 37, 380-392.
- Mattson, S.R., Gell J.W., Wilband, J.T., 1986. Chromium-rich basal pillow lavas of the Keweenawan Siemens Creek Formation, Northern Michigan. Proceedings and Abstracts of the 32nd annual Institute on Lake Superior Geology, 55.
- Meschede, M., 1986. A method of discriminating between different types of mid-ocean ridge basalts and continental tholeiites with the Nb-Zr-Y diagram. Chemical Geology, 56, 207-218.
- Miller, J.D., 1986. The geology and petrology of anorthositic rocks in the Duluth Complex, Snowbank Lake quadrangle, Northeastern Minnesota. Doctoral dissertation, 436 p.
- Minster, J.F. and Allegre, C.J., 1978. Systematic use of trace elements in igneous processes. Part III. Inverse problem of batch partial melting in volcanic suites. Contributions to Mineralogy and Petrology, 68, 37-52.
- Minster, J.F., Minster, J.B., Treuil, M., and Allegre, C.F., 1977. Systematic use of trace elements in igneous processes. Part II. Inverse problem of the fractional crystallization processes in volcanic suites. Contributions to Mineralogy and Petrology, 61, 40-77.
- O'Hara, M.J. and Mathews, R.E., 1981. Geochemical evolution in an advancing, periodically replenished, periodically tapped, continuously fractionated magma chamber. Journal of the Geologic Society of London, 138, 237-277.
- O'Hara, N.W., 1982. Great Lakes region gravity and magnetic sequence, MC-41. Geologic Society of America Map Chart Service, MC-41.
- Palmer, H.C. and Halls, H.C., 1985. The paleomagnetism of the Powder Mill Group: Its relevance to correlation with other Keweenawan sequences and to tectonic development of the south range. Abstracts for the 31st annual Institute on Lake Superior Geology, 73.

- Thompson, R.N., Dickin, A.P., Gibson, I.L., and Morrison, M.A., 1982.

  Elemental fingerprints of isotopic contamination of Hebridean
  lpaleocene mantle-derived magmas by Archean sial. Contributions to
  Mineralogy and Petrology, 79, 159-168.
- Treuil, M., 1973. Criteres petrologiques et structuraux de la genese et de la differenciation des magmas basaltiques. Exemples de l'Afar. These Orleans.
- Treuil, M. and Joron, J.L., 1975. Utilisation des elements hygromagmatophiles pour la simplification de la modelisation quantitative des processus magmatiques. Examples de l'Afar et de la dorsale methioatlantique. Society of Italian Mineralogy and Petrology, 31, 125-174.
- Wasuwanich, P., 1979. Models of basalt petrogenesis: A study of Lower Keweenawan diabase dikes and Middle Keweenawan Portage Lake Lavas, Michigan. Master's Thesis. 71 p.
- Wilband, J.T., 1984. Age and source variation of volcanics associated with Keweenawan Rifting. Transactions of the American Geophysical Union, 65, 1122.
- Wilband, J.T. and Wasuwanich, P., 1980. Models of basalt petrogenesis:

  Lower Keweenawan diabase dikes and Middle Keweenawan Portage Lake
  Lavas, Upper Michigan. Contributions to Mineralogy and Petrology, 75,
  395-406.
- Yoder, H.S., 1976. Generation of basaltic magma. National Academy of Sciences, Washington D.C. 265 p.